Eradication of Epstein–Barr Virus Episome and Associated Inhibition of Infected Tumor Cell Growth by Adenovirus Vector-Mediated Transduction of Dominant-Negative EBNA1

Md. Nasimuzzaman,[1,2,*] Masayuki Kuroda,[1,*] Sumitaka Dohno,[1] Takenobu Yamamoto,[1,3] Keiji Iwatsuki,[3] Shigenobu Matsuzaki,[1] Rashel Mohammad,[1] Wakako Kumita,[1] Hiroyuki Mizuguchi,[4] Takao Hayakawa,[5] Hiroyuki Nakamura,[6] Takahiro Taguchi,[7] Hiroshi Wakiguchi,[2] and Shosuke Imai[1,8,†]

[1]Department of Molecular Microbiology and Infections, [2]Department of Pediatrics, [6]Department of Environmental Medicine, and [7]Department of Neurobiology and Anatomy, Kochi Medical School, Kochi 783-8505, Japan
[3]Department of Dermatology, Okayama University Graduate School of Medicine and Dentistry, Okayama 700-8558, Japan
[4]Project III, National Institute of Health Sciences, Osaka Branch, Fundamental Research Laboratories for Development of Medicine, 7-6-8 Asagi, Saito, Ibaraki, Osaka 567-0085, Japan, [5]Division of Cellular and Gene Therapy Products, National Institute of Health Sciences, Tokyo 158-8501, Japan, [8]CREST, Japan Science and Technology Agency, Tokyo, Japan

*These authors contributed equally to this work.

†To whom correspondence and reprint requests should be addressed at the Program for Bio-signaling and Infection Control, Department of Molecular Microbiology and Infections, Kochi Medical School, Kohasu, Oko-cho, Nankoku, Kochi 783-8505, Japan. Fax: +81 88 880 2324. E-mail: shoimai@med.kochi-u.ac.jp.

Epstein–Barr virus (EBV) nuclear antigen 1 (EBNA1), a latent viral protein consistently expressed in infected proliferating cells, is essentially required *in trans* to maintain EBV episomes in cells. We constructed a mutant (mt) EBNA1 and examined whether it exerted dominant-negative effects on maintenance of the viral episome thereby leading to abrogation of EBV-infected tumor cell growth. Using lymphocyte and epithelial cell lines converted with neomycin-resistant recombinant EBV (rEBV) as models, adenovirus vector-mediated transduction of mtEBNA1, but not LacZ, brought about rapid and striking reductions in rEBV-derived wild-type EBNA1 levels and viral genomic loads in converted lines of three major viral latencies. This outcome was further validated at the single-cell level by cellular loss of G418 resistance and viral signals *in situ*. The mtEBNA1 transduction significantly impaired growth of naturally EBV-harboring Burkitt lymphoma cells *in vitro* and *in vivo*, largely in association with the eradication of viral episomes. Expression of mtEBNA1 per se caused no detectable cytotoxicity in EBV-uninfected cells. These results indicate that mtEBNA1 can act as a dominant-negative effector that efficiently impedes the EBV-dependent malignant phenotypes in cells regardless of viral latency or tissue origin. The mutant will afford an additional therapeutic strategy specifically targeting EBV-associated malignancies.

Key Words: Epstein–Barr virus, EBNA1 mutant, adenovirus vector, EBV episome eradication, tumor growth inhibition, gene therapy

INTRODUCTION

The Epstein–Barr virus (EBV) is a human gammaherpesvirus that can readily immortalize B lymphocytes *in vitro*, called lymphoblastoid cell lines (LCL). This immortalizing capability is relevant to understanding how EBV acts as the etiological agent of infectious mononucleosis and of often-fatal lymphoproliferative disorders in immunocompromised hosts [1]. EBV is also causally associated with endemic Burkitt lymphoma (BL) and undifferentiated nasopharyngeal carcinoma [1]. Over the past 15 years the array of human cancers potentially related to EBV has increased and now includes Hodgkin disease, subgroups of T or natural killer (NK) cell lymphoma, and gastric carcinoma [1–6].

These EBV-associated malignant diseases are clinically aggressive and often less responsive to conventional

therapy, and currently available anti-herpesvirus (lytic-cycle) drugs are ineffective treatments. A unique *in vivo* feature of EBV-associated malignancies is consistent existence (generally monoclonal) and expression of EBV exclusively in tumor cells and not in surrounding normal cells. In addition, considerable evidence has shown that EBV itself and some of its virus-encoded latent genes are actually implicated in certain critical aspects of the oncogenic event in cells [8–18]. These facts, therefore, give enough scope for exploitation of tumor-specific gene therapy that can eliminate EBV itself from malignant cells.

EBV usually persists as a circular extrachromosomal episome in latently infected LCL, or tumor cells (multi-copies per cell in general), in which viral latent genes are expressed in different combinations, generally dependent upon the cell/tumor type [1,7]. The major EBV latent genes include six nuclear antigens (EBNAs 1–6), three latent membrane proteins (LMPs1, 2A, and 2B), two small nonpolyadenylated RNAs (EBERs 1 and 2), and the somewhat complex *Bam*HI-A rightward transcripts (so-called BARTs or CSTs) [7]. Latent EBV infection in dividing cells *in vitro* and *in vivo* is classified into three types according to patterns of latent gene expression: Latencies I, II, and III. A full set of the latent genes is expressed in Latency III, typified by LCL, whereas a restricted set is expressed in Latencies I and II, which are represented by BL and T/NK cell lymphoma, respectively [1].

Of the EBV latent genes, EBNA1 is commonly expressed in EBV-infected proliferating cells irrespective of latency type and tissue origin, although three EBNA transcriptional promoters localized in the *Bam*HI-C, -W, and -Q regions of the EBV genome (Cp, Wp, and Qp, respectively) are differentially utilized [7,19,20]. Biologically, the EBNA1 protein has functional plasticity, as indicated by its role as a transactivator required for viral episome maintenance within cells (replication upon cell division and segregation into daughter cells) and as a transcriptional enhancer for Cp, Wp, and the LMP1/2B

promoter via binding to *cis*-acting elements of the latent viral replication origin, *ori*P, in Latency III [21–24]. EBNA1 also participates in the regulation of Qp through binding to a cognate sequence adjacent to Qp in Latencies I and II [25]. Furthermore, EBNA1 may be involved in regulating other genes, transcriptionally or posttranscriptionally, via its protein-binding and/or putative RNA-binding properties or an undefined mechanism(s) [12,26–30]. EBNA1 also elicits immune T cell responses, thereby activating production of some cytokines by T cells, and this, in turn, would promote EBV-infected cell proliferation [31].

Many studies have clarified the precise intramolecular location and functions of some of the domains of the EBNA1 protein [7,22,30,32–34]. Based on domain mapping data, the present study constructed a mutant (mt) EBNA1 gene lacking the most N-terminal half, relative to wild-type (wt) EBNA1, and incorporated it into a conventional replication-incompetent adenovirus serotype 5 vector (Adv5) [35] or its fiber-substituted variant (Adv5/35f) [36]. Utilizing these recombinant adenovirus vectors (Adv's), we examined whether this mtEBNA1 could interrupt the maintenance of EBV episomes in latently infected tumor cells. The results indicated, for the first time, that Adv-mediated transduction of the mtEBNA1 efficiently eradicated viral episomes from cells regardless of viral latency type, tissue origin, or virus strain. Consequently, cellular loss of EBV executed by our mtEBNA1, referred to as dominant-negative (dn) EBNA1, caused remarkable growth inhibition of naturally virus-harboring BL tumor cells. Thus, the dnEBNA1 will provide the basis for a novel, reasonable therapeutic molecule specifically directed against EBV-associated malignancies.

RESULTS

Infection of Cell Lines by Adv

We examined the human cell lines used in this study (Table 1) for efficiency of Adv-mediated gene transfer

TABLE 1: Susceptibility of cell lines to Adv

Cell line	Cell type/EBV latency	%EGFP-positive cells[a] (applied m.o.i. of Adv)						
		1	2	5	10	20	50	70
Akata⁻/rEBV[b]	B cell/Latency I	45.7	55.1	59.5	67.2	84.0	84.5	85.3
MT-2/rEBV[b]	T cell/Latency II	–	–	85.3	85.3	91.2	94.0	ND
BJAB/rEBV[b]	B cell/Latency III	–	–	48.2	48.2	65.8	83.9	89.8
NU-GC-3/rEBV[b]	Epithelium/Latency I	–	–	74.1	82.5	92.8	94.7	95.8
Mutu I[c]	B cell/Latency I	53.2	59.1	59.8	64.7	63.5	63.9	ND
Akata-EC[c]	B cell/Latency I	34.2	41.5	52.4	60.4	56.2	ND	ND
MRC-5[d]	Fibroblast	–	–	49.3	62.9	78.6	88.9	ND

[a] Flow cytometric analysis data are presented as a percentage of enhanced green fluorescent protein (EGFP)-positive cells over background (control Adv-LacZ inoculation at the same multiplicity of infection (m.o.i.)). Data represent the means of three independent assays performed on each cell line (SD was <6% in all cases). Results obtained using one of the four kinds of Adv's (see Materials and Methods) that produced the highest infectivity are shown here, i.e., Adv5-CV-EGFP for the NU-GC-3/rEBV cell line, Adv5/35f-SV-EGFP for the MRC-5 cell line, and Adv5-SV-EGFP for the other cell lines. Cells were analyzed 3 days after Adv inoculation. –, not tested; ND, not determined due to appearance of significant cytotoxicity caused by Adv-LacZ.
[b] rEBV-converted or -reinfected cell lines.
[c] Naturally occurring BL cell lines.
[d] Human fibroblast.

using purified Adv's for enhanced green fluorescent protein (EGFP) expression, Adv5-EGFP and Adv5/35f-EGFP (the simian virus 40 early promoter (SVp)-driven and the cytomegalovirus early promoter (CMVp)-driven for each Adv type). Flow cytometric analysis revealed that all cell lines attained maximal EGFP-positive signal of 50–95% for at least one of the four kinds of Adv's (see Materials and Methods) at m.o.i. ranging from 5 to 70 (Table 1). According to these results, we selected an Adv (and promoter) type suitable for each cell line and used it for the following experiments.

Adv-Mediated Expression of mtEBNA1

We checked isolated Adv clones confirmed to be carrying the mtEBNA1 or wtEBNA1 gene construct (Fig. 1) for expression of these proteins by immunoblotting. Representative results of Adv5-CV-DNE1 and Adv5-CV-AKE1 clones (for designation of Adv's, see Materials and Methods) are shown in Supplemental Fig. S1. We probed blots with EBV-positive reference human serum and detected an 82-kDa band, indicative of wtEBNA1 (Akata strain [37]), only in cells inoculated with Adv5-CV-AKE1, which served as the positive control. On the same blots, we detected a signal band at around 21 kDa, the expected molecular size of mtEBNA1, in cells inoculated with Adv5-CV-DNE1 but not with Adv5-CV-LacZ (Supplemental Fig. S1). The 21-kDa band was also produced by clones of Adv5-SV-DNE1, Adv5/35f-CV-DNE1, and Adv5/35f-SV-DNE1 (data not shown). Neither the 21-kDa nor the 82-kDa protein was detectable when probed with EBV-negative human serum (data not shown).

Reduction of Episome-Derived wtEBNA1 Expression and EBV Genomic Loads by mtEBNA1 Transduction

We analyzed the effects of mtEBNA1 using EBV-converted or -reinfected cell lines (Table 1), which had been established in vitro by infecting virus-negative cells with recombinant EBV (rEBV; Akata strain) that carries the neomycin-resistance gene (neo^r) as a selective marker [38]. For example, we cultured the rEBV-converted epithelial cell line NU-GC-3/rEBV [39] in the absence of G418 for 7 days and inoculated it with Adv5-CV-DNE1 and monitored the expression of both rEBV episome-derived wtEBNA1
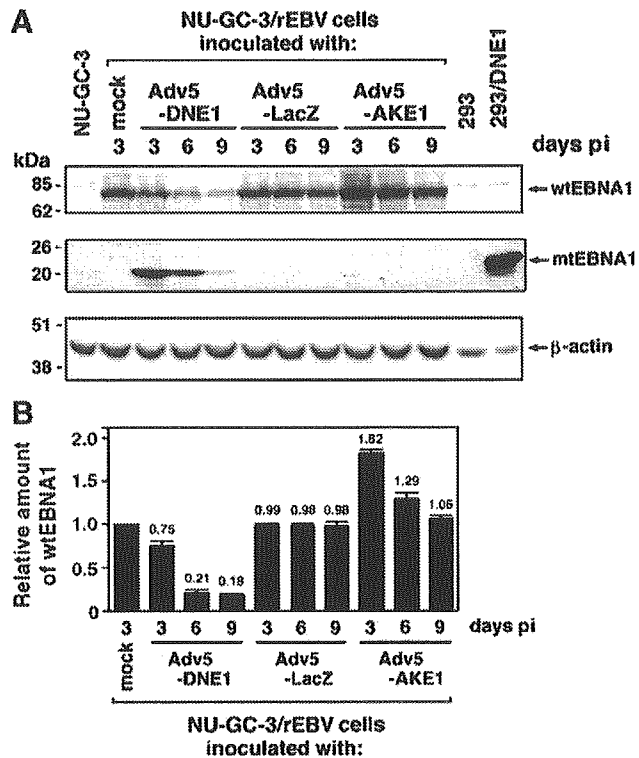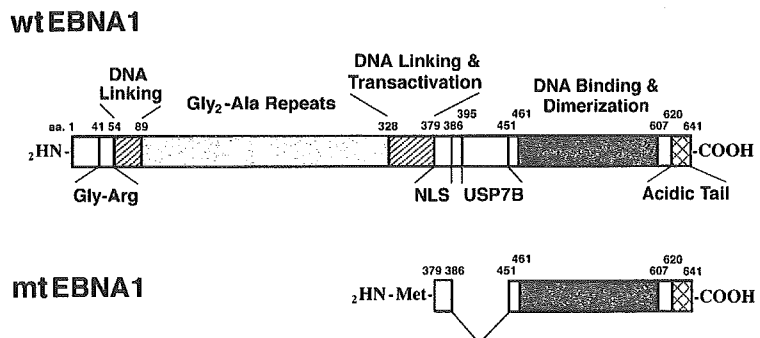

FIG. 2. Sequential decrease in rEBV episome-derived wtEBNA1 expression by mtEBNA1 transduction. (A) Immunoblot. Representative data from one of three experiments using the epithelial converted cell line NU-GC-3/rEBV are shown. Cells were inoculated with CsCl-purified Adv5-CV-DNE1 or -LacZ or -AKE1 (m.o.i. of 20) and cultured without G418. Expression of wtEBNA1 (top row), mtEBNA1 (second row), and β-actin (third row) was assayed at the days indicated postinoculation (pi). The cell lines 293 and 293/DNE1 served as mtEBNA1-negative and -positive cell controls, respectively (see Materials and Methods). Molecular size standards are indicated at the left. (B) Quantification of wtEBNA1 expression levels. Bands specific for wtEBNA1 were analyzed quantitatively in comparison with β-actin signals. Expression levels of wtEBNA1 protein in the Adv5-CV-DNE1- or Adv5-CV-LacZ-inoculated NU-GC-3/rEBV cells were expressed as relative values against a mock-infected control. Black columns with bars represent means ± SD of results from three repeated experiments.

and transduced mtEBNA1 proteins by immunoblotting. The 21-kDa mtEBNA1 protein was detectable at least for 9 days after Adv inoculation (Fig. 2A). Concomitantly, expression of wtEBNA1 prominently declined with time

FIG. 1. Structure of mtEBNA1 used in this study. Functional domains of the mtEBNA1 are schematically diagramed in comparison with wtEBNA1. Amino acid coordinates are indicated above the limits (vertical bars) of each domain according to the published data [22,30,34]. The coding constructs of mtEBNA1 and wtEBNA1 (LacZ and EGFP, too), which are transcribed by SVp or CMVp, were incorporated into Adv5 or Adv5/35f. NLS and USP7B indicate nuclear localization signal [22] and putative ubiquitin-specific protease 7 binding domain [30], respectively.

(Fig. 2A). A quantitative analysis, normalized to β-actin levels, demonstrated that wtEBNA1 expression from Adv5-CV-DNE1 inoculation, but not in Adv5-CV-LacZ inoculation, decreased to 75 and 18% of the mock-inoculated control 3 and 9 days after inoculation, respectively ($P <$ 0.01, analyzed by ANOVA, followed by the post hoc Tukey test) (Fig. 2B). We also observed a similar reduction in wtEBNA1 in other rEBV-reinfected and -converted lym-
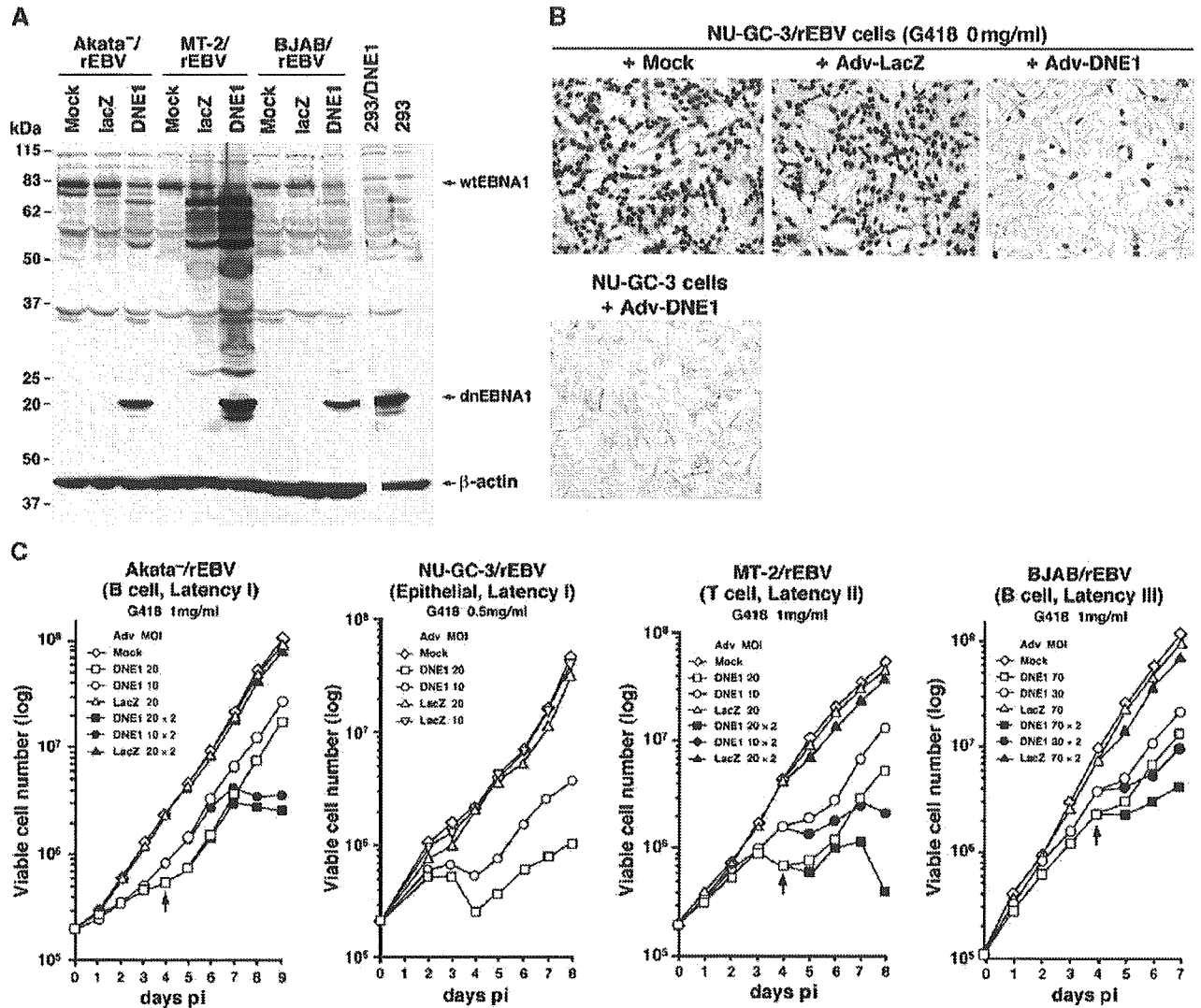

FIG. 3. Complete eradication of EBV episomes by dnEBNA1 at the single-cell level regardless of latency type and cell type. (A) Expression of dnEBNA1 in other rEBV-converted cell lines. Substantial expression of dnEBNA1 (hereafter, our mtEBNA1 is referred to as "dnEBNA1," see text) in rEBV convertants of different EBV latency types and cell lineages (Table 1). Results from Akata⁻/rEBV, MT-2/rEBV, and BJAB/rEBV are shown. The convertants were inoculated with Adv5-SV-DNE1 at an m.o.i. of 20 for Akata⁻/rEBV and MT-2/rEBV and 70 for BJAB/rEBV and cultured without G418. Immunoblot analysis was carried out 3 days postinoculation. Obvious 21-kDa bands, indicative of dnEBNA1, and a decrease in 82-kDa bands representing wtEBNA1 were unequivocally seen only in Adv5-SV-DNE1-inoculated cells. Several accentuated extra bands, particularly visible in MT-2/rEBV cells exposed to Adv, could represent adenovirus-related proteins that reacted with human serum used as the probe. Detection of β-actin levels served as the internal control. The negative and positive controls, 293 and 293/DNE1, respectively, are the same as explained in the Fig. 2A legend. Molecular size standards are indicated on the left. (B) EBER1-ISH. Representative data from a series of NU-GC-3/rEBV cells are shown. The cells were inoculated with Adv's at an m.o.i. of 20 and cultured in the absence of G418. The incidence of rEBV loss was assessed by EBER1-ISH 9 days after inoculation. Cells with strong nuclear signals are EBER1-positive. NU-GC-3 + Adv5-DNE1 served as a rEBV-negative control. Fine granular precipitates visible in the background of Mock and Adv5-LacZ samples of NU-GC-3/rEBV are nonspecific products that occasionally appear during the final chromogenic reaction step. Original magnification: ×100. (C) Growth kinetics of dnEBNA1-transduced rEBV convertants in the presence of G418. Adv5-CV-DNE1 or -LacZ was used for NU-GC-3/rEBV and Adv5-SV-DNE1 or -LacZ was used for the other convertants. The Adv's and applied m.o.i. are indicated by abbreviations and Arabic numerals, respectively, and are attached to the symbols. In Akata⁻/rEBV cells, for example, DNE1 20 represents a single Adv5-SV-DNE1 inoculation at an m.o.i. of 20, and DNE1 20 × 2 represents repeated Adv5-SV-DNE1 inoculations at an m.o.i. of 20. The second Adv inoculation is indicated by an arrow. Viable cells were consecutively counted by trypan blue dye exclusion. Data from one of two independent experiments are provided here.

phoid lines exposed to Adv5-SV-DNE1 (Fig. 3A). The marked decrease in wtEBNA1 expression by mtEBNA1 transduction could represent elimination of rEBV episomes from a considerable fraction of cells, although the possibility that wtEBNA1 expression was down regulated by mtEBNA1 cannot be excluded at this step.

To investigate whether mtEBNA1 inhibits rEBV episome maintenance in cells, we quantified viral genomic DNA loads sequentially by real-time PCR after Adv inoculation. We exposed NU-GC-3/rEBV cells to Adv likewise and then cultured them in the absence of G418. rEBV genome loads in Adv5-CV-DNE1-exposed cells began to decrease 3 days postinoculation and were considerably reduced to 11% of the Adv5-CV-LacZ-exposed control 9 days postinoculation (Table 2). In contrast, the dynamics of viral genome loads in Adv5-CV-LacZ inoculation was unchanged throughout the observation (Table 2). Immunofluorescent staining consistently showed that more than 98% of cells exposed to Adv5-CV-LacZ, or mock infected, were positive for wtEBNA1 26 days after removal of G418 from culture (data not shown), indicating that spontaneous loss of the rEBV genome was not frequent, even in G418-free culture during the test period. Reduction of rEBV loads by mtEBNA1 transduction occurred in Akata⁻/rEBV cells [14] as well (a decrease to 19% of the LacZ control, Table 2; for mtEBNA1 expression, see Fig. 3A). Thus, our mtEBNA1, as a dominant-negative EBNA1, can efficiently eradicate viral episomes from cells, at least at the bulk-culture level.

dnEBNA1-Induced Eradication of EBV Episomes at Single-Cell Level in Different EBV Latency Programs and Tissue Origins

We then examined whether dnEBNA1 could efficiently eradicate EBV episomes (multicopies per cell) at the single-cell level by in situ hybridization for EBV-encoded small RNA 1 (EBER1-ISH) using rEBV-converted cell lines, since our previous study [39] demonstrated that an EBER expression status correlates well with the rEBV genome persistence/loss in converted cells. Adv5-SV- (or -CV)-

DNE1 also successfully expressed dnEBNA1 protein at substantial levels in the other converted lines, MT-2/rEBV (T cell) [40] and BJAB/rEBV (B cell) [41] (Fig. 3A; the decrease in wtEBNA1 levels should also be noted), which display EBV latency types II and III, respectively (Table 1). EBER1-ISH showed that 89 ± 3% of NU-GC-3/rEBV cells (Fig. 3B), 77 ± 5% of Akata⁻/rEBV cells, 80 ± 6% of BJAB/rEBV cells, and 85 ± 3% of MT-2/rEBV cells in the absence of G418 appeared to be negative for EBER1 9 days after a single inoculation with Adv5-SV- (or -CV)-DNE1. These reproducible findings were reflected also by looking at the growth kinetics of rEBV-converted cell lines in the presence of G418. The experimental concept is based on the premise that cells that lose rEBV (rEBV-lost cells) cannot survive in G418-containing culture [38,39]. The Adv5-SV (or -CV)-DNE1-exposed cultures showed obvious, albeit transient, suppression of cell proliferation 4 to 6 days postinoculation, whereas Adv5-SV (or -CV)-LacZ-exposed cells as well as mock-infected controls continued to grow steadily (Fig. 3C). The loss of resistance to G418 cytotoxicity occurred dose dependently upon addition of Adv5-DNE1, and the maximal growth inhibition achieved by a single Adv5-DNE1 inoculation was almost equal among all the converted cell lines. The viability was 9–23% of the corresponding Adv5-LacZ-inoculated controls (Fig. 3C) and is largely consistent with the ability of Adv's to infect the convertants (Table 1). After the "nadir" of cell viability, as was typically seen in NU-GC-3/rEBV, dnEBNA1-transduced cultures were liberated from growth suppression 6 days after a single Adv inoculation (Fig. 3C), representing a proliferation of cells that still carried rEBV, i.e., cells not transduced with the dnEBNA1 gene. When we reexposed cells to Adv5-SV-DNE1 4 days after the first inoculation, their growth was more affected (Fig. 3C).

The results indicated overall that our dnEBNA1 did eliminate multiple rEBV episomes almost completely at the single-cell level from individual cells into which dnEBNA1 was successfully transduced, in any major viral latency and in different cell backgrounds.

TABLE 2: Reduction of rEBV genomic loads by mtEBNA1 transduction

Cells	Inoculation	EBV genome number per cell[a] (days after Adv inoculation)				
		0	3	6	9	12
NU-GC-3/rEBV	Mock	1.9 ± 0.36	1.9 ± 0.20	1.8 ± 0.29	1.8 ± 0.26	NT
	Adv5-CV-LacZ		1.8 ± 0.12	1.7 ± 0.18	1.8 ± 0.11	NT
	Adv5-CV-DNE1		0.9 ± 0.12	0.3 ± 0.23	0.2 ± 0.04	NT
Akata⁻/rEBV	Mock	26.7 ± 3.2	24.8 ± 1.2	25.0 ± 0.8	26.6 ± 1.2	25.4 ± 1.9
	Adv5-SV-LacZ		26.1 ± 2.5	28.0 ± 2.6	28.3 ± 1.7	24.9 ± 2.1
	Adv5-SV-DNE1		22.3 ± 0.6	15.8 ± 2.2	5.0 ± 0.3	6.1 ± 0.7
Namalwa[b]	–	2.0 ± 0.08				
BJAB[b]	–	0				

[a] Viral genome copies per cell were quantified by the real-time PCR assay after Adv-mediated mtEBNA1 transduction. In the experiments, G418 was removed from culture 7 days before Adv inoculation, and 0.1 mM acyclovir (an inhibitor of viral genome amplification during the lytic cycle) was added to the culture 3 days before Adv inoculation (m.o.i. of 20) to prevent overestimation of latent viral episome number, which may be caused by the possibly occurring spontaneous viral lytic cycle. Data indicated are averages ± SD of results from three experiments. NT, not tested.

[b] Namalwa [65] and BJAB cells served as EBV-positive and -negative controls, respectively, for each test, and the results were highly reproducible.

Therapeutic Potential of dnEBNA1 Against Naturally EBV-Infected BL Cells

We assessed dnEBNA1 for its ability to inhibit the growth of naturally EBV-infected BL tumor cells in association with the enforced loss of resident viral episomes using Mutu I [42] and Akata-EC (early cultured) cells [17]. We selected these BL cells as test cells because (1) EBV-lost clones of Mutu I cells can be isolated spontaneously or by chemical treatment (at a low frequency) and can still survive, although these clones reportedly exhibit impaired growth [16,43], and (2) the survival/growth of Akata-EC cells strongly depends on the existence of EBV [17]. After Adv5-SV-DNE1 inoculation at an optimal m.o.i., dnEBNA1 protein was expressed in Mutu I cells at significant levels and in Akata-EC cells at a detectable level but at a level noticeably lower than in the Mutu I cells (Fig. 4A). The expression of wtEBNA1 was clearly decreased in the Mutu I cells (Fig. 4A), as seen in rEBV-converted cells (Figs. 2 and 3A). In contrast, unexpectedly, the wtEBNA1 expression level in Akata-EC cells exposed to Adv5-SV-DNE1 remained unchanged (Fig. 4A). Consistently, quantitative PCR assay showed that EBV DNA loads decreased significantly in the Mutu I cells, but were almost unchanged in Akata-EC cells after exposure to Adv5-SV-DNE1. The virus genome copy numbers per Mutu I cell after 6 days were 11.2 ± 4.6 following Adv5-SV-DNE1 inoculation vs 39.8 ± 3.5 in Adv5-SV-LacZ inoculation controls and 42.0 ± 2.6 in mock-inoculated cells ($P < 0.01$). However, successive viable cell counts monitored in parallel revealed that Adv5-SV-DNE1 significantly suppressed the growth of both Mutu I and Akata-EC BL lines in a dose-dependent fashion, compared with Adv5-SV-LacZ-inoculated cells ($P < 0.001$) (Fig. 4B). These results suggest that most EBV-lost Mutu I cell clones were still living but underwent profound growth retardation [16,43], whereas Akata-EC clones were more likely to have been predisposed to immediate cell death rather than growth arrest after EBV was eradicated [17].

To corroborate that dnEBNA1 truly eradicated EBV episomes from naturally EBV-positive BL cells at the single-cell level, we exposed Mutu I cells to Adv's for the picornavirus intraribosomal entry site (IRES)-mediated coexpression of dnEBNA1 or LacZ with hygromycin B resistance (hyg^r), i.e., Adv5-SV-DIH or -LIH (Fig. 4C; for designation of Adv's, see Materials and Methods), and then cultured them in the presence of hygromycin B to grow selectively cells expressing dnEBNA1 or LacZ (the selection conditions are detailed in the legend to Fig. 4D). The fluorescence *in situ* hybridization (FISH) assay demonstrated that >96% of Adv5-SV-DIH-inoculated/hygromycin B-selected viable Mutu I cells were negative for EBV genomic signals 10 days after Adv inoculation (Fig. 4D, bottom left), whereas ≤0.3% of Adv5-SV-LIH-inoculated/hygromycin B-selected viable cells were negative for these signals (Fig. 4D, bottom middle) ($P < 0.001$ by t test). These results signify that individual cells that were transduced with dnEBNA1 lost multiple copies of the EBV episome. Without hygromycin B treatment, 59% of the Mutu I cells in Adv5-SV-DIH-inoculated culture were negative for FISH signals (Fig. 4D, top middle) vs 0.4% in Adv5-SV-LIH-inoculated culture (Fig. 4D, top right) ($P < 0.001$) 10 days after Adv inoculation, indicating that the positive selection worked well. In contrast, FISH-negative cells were detected only in a small population (≤7%) of Akata-EC cells after Adv5-SV-DNE1 inoculation, which was compatible with the results of immunoblots (Fig. 4A) and quantitative PCR assays (see above). In cell-sorting experiments, as expected, sufficient viable Akata-EC cells for analysis were obtained from Adv5-SV-LIH-inoculated/hygromycin B-selected control culture, but not from Adv5-SV-DIH-inoculated/hygromycin B-selected culture, suggesting again that most EBV-lost Akata-EC clones by dnEBNA1 were not able to survive [17].

Influence of dnEBNA1 on EBV-Uninfected Cells

We further examined whether dnEBNA1 would cause any adverse effects on EBV-uninfected nonmalignant cells (i.e., the human fibroblasts, MRC-5) and pairs of EBV-negative tumor lines and their virus convertants. Inoculation of MRC-5 with the fiber-substituted Adv5 vector [36] Adv5/35f-CV-DNE1 gave rise to dnEBNA1 expression levels consistent with a high efficiency of gene transfer (~75% of cells, Table 1) sufficient to assess the effects of dnEBNA1 on cell growth (Fig. 5A, left). MRC-5 cells inoculated with Adv5/35f-CV-DNE1 did not differ in growth characteristics from the Adv5/35f-CV-LacZ-inoculated control ($P = 0.386$) (Fig. 5A, right). Similarly in the EBV-negative NU-GC-3 line, Adv5-CV-DNE1 inoculation caused no significant difference in growth compared with the control Adv5-CV-LacZ inoculation ($P = 0.846$) (Fig. 5B, left). On the other hand, in the rEBV-convertant NU-GC-3/rEBV line, Adv5-CV-DNE1 inoculation significantly suppressed growth in comparison with Adv5-CV-LacZ inoculation ($P < 0.01$) (Fig. 5B, right). This growth suppression was considered to be attributable to dnEBNA1-induced eradication of rEBV, rather than cytotoxicity induced by dnEBNA1 per se, because dnEBNA1-transduced NU-GC-3/rEBV (with >90% of cells that lost rEBV, as shown in Fig. 3B) revealed a growth pattern similar to that of its parental (virus-negative) NU-GC-3 cell line (Fig. 5B, left). Consistent with these data is our previously reported result [15] that the growth of NU-GC-3 cells is promoted by conversion with rEBV. Transduction of dnEBNA1 did not affect the growth of other EBV-negative cell lines such as Akata⁻ and BJAB (data not shown).

Suppressive Effect of dnEBNA1 on Tumor Growth/Induction *in Vivo*

Finally, we examined the *in vivo* effects of dnEBNA1 using an animal xenograft model. When subcutaneous
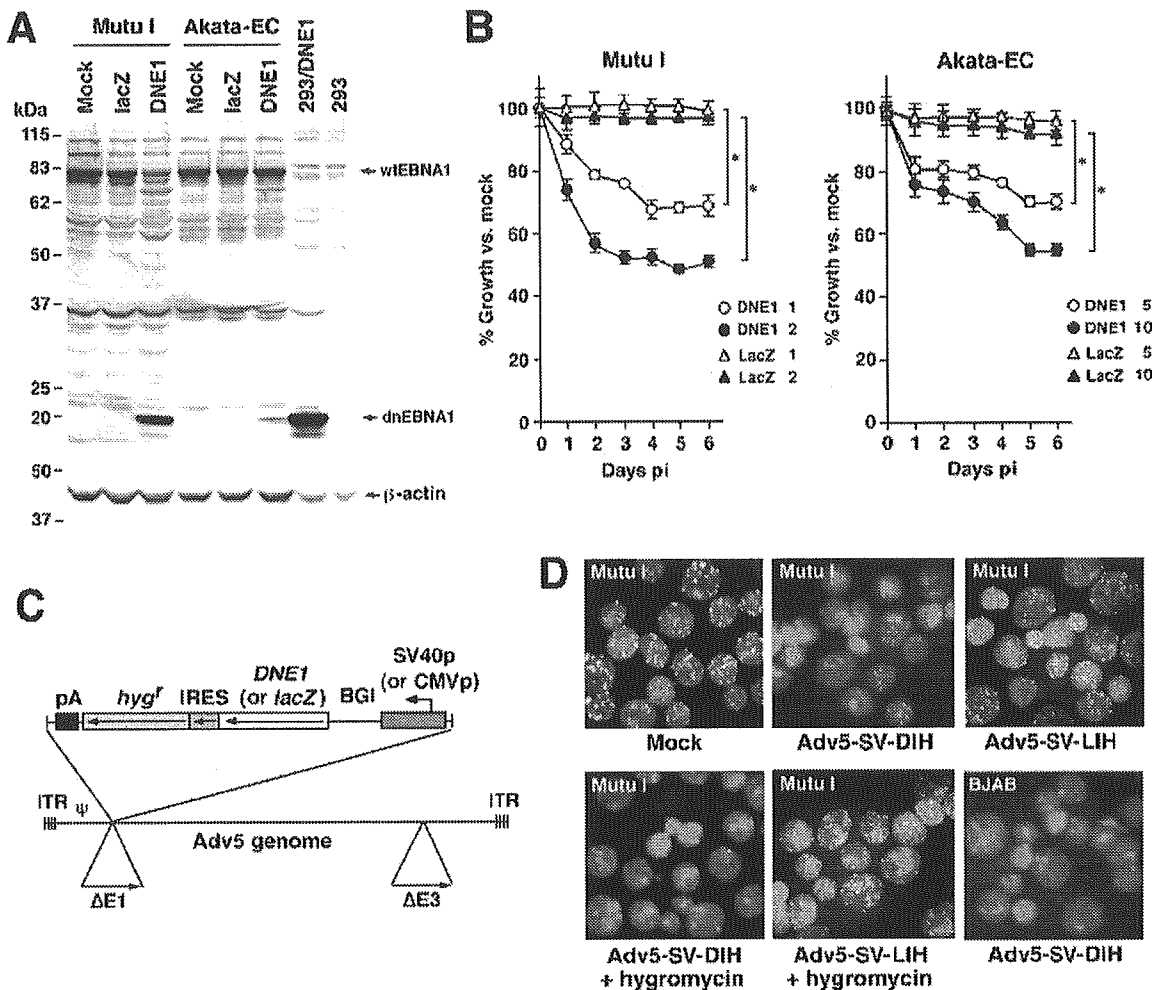
FIG. 4. Effects of dnEBNA1 on naturally EBV-positive BL tumor cells. (A) Immunoblot analysis of dnEBNA1 transduction. Applied m.o.i. of Adv5-SV-DNE1 or -LacZ were 2 for Mutu I and 10 for Akata-EC. 293/DNE1 indicates a positive control for dnEBNA1 expression. Expression of wtEBNA1 and dnEBNA1 (top), along with that of β-actin as an internal control (bottom), was assayed at 4 days after Adv inoculation. Molecular size standards are indicated on the left. (B) Cell proliferation assay. Mutu I or Akata-EC cells were inoculated with Adv's, at different m.o.i. as indicated by the symbols, and their growth was followed by WST-1 assay, which was started 5 h after Adv inoculation (Day 0). Results are expressed as a percentage of absorbance values of Adv5-SV-DNE1- (circles) or Adv5-SV-LacZ-inoculated cultures (triangles) against the absorbance of the mock-infected control on each day. DNE1 2, for example, represents inoculation with Adv5-SV-DNE1 at an m.o.i. of 2. Each symbol with a bar represents mean ± SD of the absorbance percentages obtained from the experiments repeated three times. ANOVA showed significant main effects of Adv-DNE1 inoculation (*). Post hoc Dunnett test revealed a significant decrease in percentage values against mock-infected cells in cells inoculated with Adv5-SV-DNE1 at both m.o.i. (C) Adv construct for bicistronic gene expression. The genome structure of Adv5-SV (or -CV)-DIH (or -LIH) used to sort gene-transduced cells is schematically shown. BGI, β-globin intron sequence; IRES, intraribosomal entry site; ITR, adenoviral inverted terminal repeat; ψ, packaging signal; pA, poly(A) signal; ΔE1 and ΔE3, deleted genes in the vector genome [35]. (D) FISH analysis of EBV genome. Data from a series of Mutu I cells are shown. Adv5-SV-DIH and -LIH denote inoculations with Adv's for dual expression of dnEBNA1 or LacZ, respectively, along with hygʳ as the selective marker. Mutu I, Adv5-SV-DIH + hygromycin and Mutu I, Adv5-SV-LIH + hygromycin denote cultures that were inoculated with Adv (m.o.i. of 2) and then treated with hygromycin B (400 μg/ml) to remove cells that had not been transduced with the genes. Hygromycin B was added to culture on the day following Adv inoculation, and then cells were cultivated for 4 consecutive days. The resultant surviving cells were propagated in the absence of hygromycin B for a further 5 days and screened for EBV infection by FISH. Mutu I, Adv5-SV-DIH and Adv5-SV-LIH denote cultures inoculated with Adv alone. Mutu I, Mock and BJAB, Adv5-SV-DIH served as EBV-positive and -negative controls, respectively. All samples were assessed 10 days postinoculation. Cells with green fluorescent dot signals are positive for the EBV genome. Original magnification: ×200.

tumors appeared in 24 flanks of 12 SCID mice tested after implantation of Mutu I cells (for details of procedure, see Materials and Methods)—usually at 9–11 days—we gave intratumoral injections with Adv5-SV-DNE1, Adv5-SV-LacZ, or phosphate-buffered saline (PBS) in 8 flanks each and observed the animals for up to 14 days after injection. During this time, all 8 tumors injected with Adv5-SV-DNE1 ceased to grow or
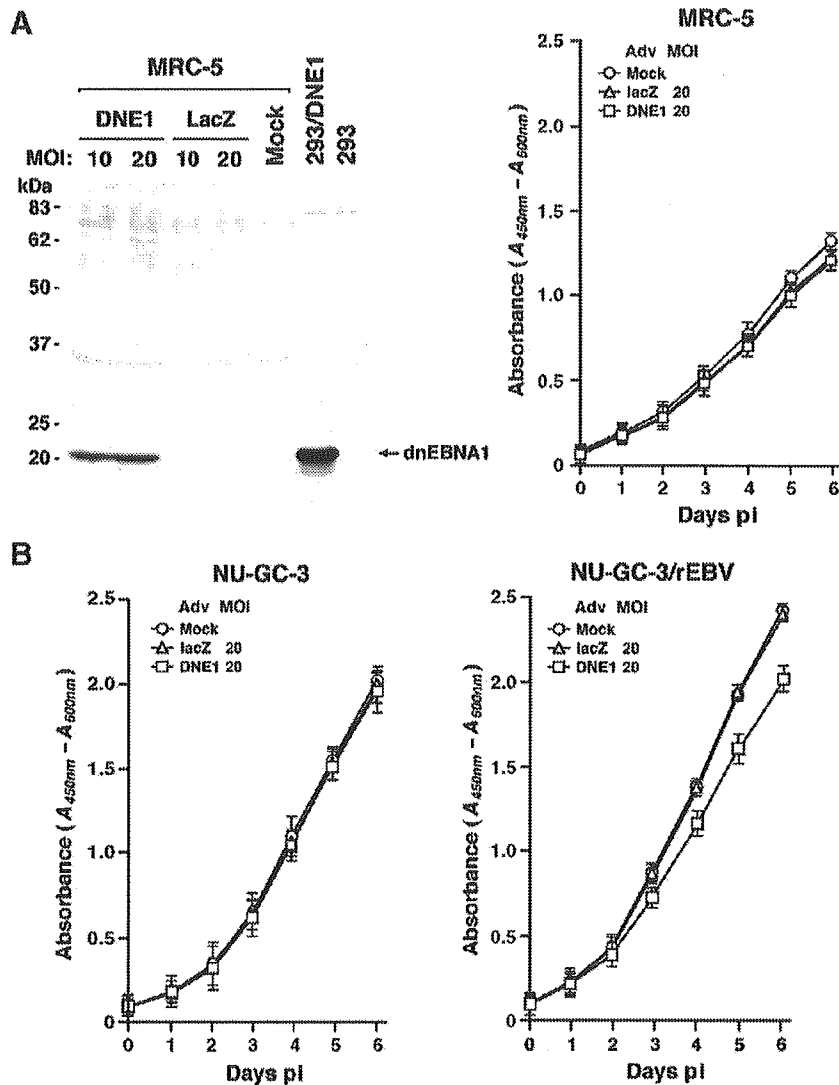
FIG. 5. Effects of dnEBNA1 on EBV-uninfected cells. (A) Adv-mediated dnEBNA1 expression and its effect on MRC-5 cell growth. MRC-5 cells were inoculated with Adv5/35f-CV-DNE1 or -LacZ at m.o.i. of 10 and 20 and analyzed by immunoblotting 3 days postinoculation (pi) (left). 293/DNE1 and 293 indicate the positive and negative controls, respectively. Molecular size standards are indicated at the left. Proliferation of MRC-5 cells (right) was measured by WST-1 assay after Adv5/35f-CV-DNE1 or Adv5/35f-CV-LacZ inoculation at the indicated m.o.i., compared with mock infection. Day 0 represents 5 h after Adv inoculation. Each symbol with a bar represents mean ± SD of the absorbance obtained from one of three experiments. Statistical analysis was carried out as done for Fig. 4B. (B) Proliferation of the NU-GC-3 line (left) and its rEBV-convertant NU-GC-3/rEBV (right) after dnEBNA1 transduction. Cells (6 × 10^2/well) were inoculated with Adv5-CV-DNE1 or Adv5-CV-LacZ at the indicated m.o.i. The substantial Adv-mediated expression of dnEBNA1 in both cell lines was as shown in Supplemental Fig. S1 and Fig. 2. Cell growth was measured by WST-1 assay in comparison with mock infection. Day 0 represents 5 h after Adv inoculation. Data are expressed as in (A) and were statistically analyzed as done for Fig. 4B.

regressed (1 tumor), whereas the 16 tumors injected with Adv5-SV-LacZ or PBS continued to grow aggressively (Fig. 6A). This was confirmed by the significant difference in tumor weights between the dnEBNA1-transduced mouse group and the control groups ($P <$ 0.001 by Mann–Whitney U test) (Fig. 6B). EBER1-ISH and histological examinations showed that EBV-lost cells (~30%) and dead cells were present in the small tumors at the Adv5-SV-DNE1 inoculation sites, and the large tumors at the control sites were filled with viable EBER1-positive cells (data not shown). Another animal experiment revealed that implantation of Mutu I cells preinoculated with Adv5-SV-DNE1 did not induce tumors at all in all four tested flanks of mice, but implantation of cells preinoculated with Adv5-SV-LacZ induced tumors in all four implanted flanks that exceeded 2 cm in dimension by 14–20 days after cell

injection (Fig. 6C). These results indicate that dnEBNA1 acts to suppress tumor growth in vivo.

DISCUSSION

A previous study by others has shown that several EBNA1 derivatives are capable of interrupting the EBNA1-oriP functions, using an artificial system of oriP-carrying plasmids and cells transfected with the wtEBNA1 gene [34]. In the present study we have demonstrated that an EBNA1 mutant, with a similar domain constitution, eradicates EBV episomes efficiently from infected cells, therefore acting as dnEBNA1, irrespective of viral latency type and cell lineage (lymphoid and epithelial). In fact, transduction of dnEBNA1 yielded EBV-negative cell clones from naturally EBV-infected BL lines Mutu I and Daudi at a much
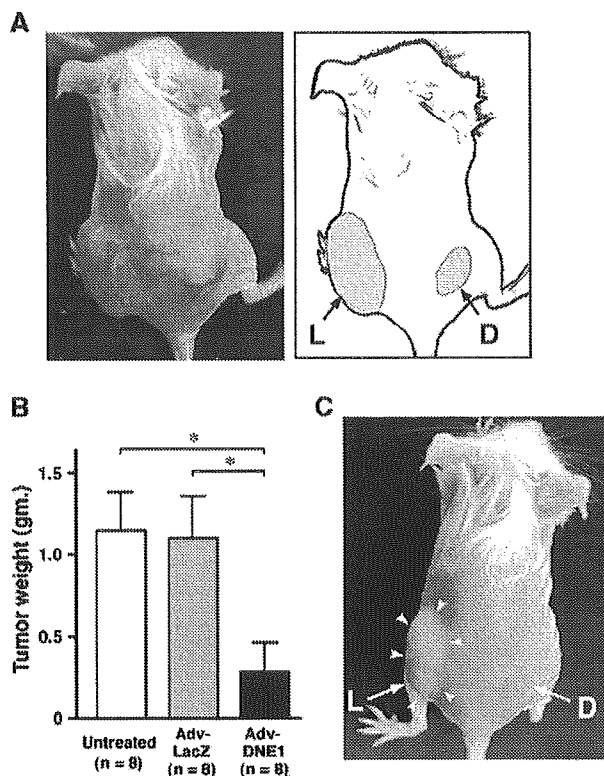
FIG. 6. Animal experiments. (A) Inhibition of tumor growth by dnEBNA1. Mutu I cells (1 × 10^7) were implanted subcutaneously in each flank of 12 SCID mice (i.e., 24 flanks). When tumors became palpable, at about 10 days after implantation, Adv's (10^8 pfu per dose) and PBS (mock) were injected into 8 tumors each. A representative result photographed 8 days after Adv inoculation (i.e., 17 days after cell implantation) is shown here. The sites of Adv5-SV-DNE1 and Adv5-SV-LacZ injections are indicated on the mouse flank by D and L, respectively. (B) Changes in tumor size. The procedures and subjects used for experiment are the same as in (A). Each column with a bar represents the mean ± SD of weight (in grams) of tumors resected from each SCID mouse group, comprising 8 tumors in their flanks. Untreated, Adv-LacZ, and Adv-DNE1 represent intratumoral injections with PBS, Adv5-SV-LacZ, and Adv5-SV-DNE1, respectively. A statistically significant difference in tumor weight between the mouse groups is shown by asterisks. (C) Inhibition of tumor induction. Mutu I cells (1 × 10^7) preexposed to Adv5-SV-DNE1 or Adv5-SV-LacZ (m.o.i. of 2) were implanted subcutaneously in both flanks of each of four SCID mice, and tumor formation was observed. D and L indicate the implantation sites of Adv5-SV-DNE1- and Adv5-SV-LacZ-preexposed cells, respectively. A representative result photographed 14 days after cell implantation is shown.

higher frequency than that of spontaneous isolation (our unpublished data), suggesting that the dnEBNA1 acts effectively not only against the common laboratory strain of EBV such as Akata, but also against other wild strains. Accordingly, the dnEBNA1 may facilitate the rapid in vitro production of an isogenic pair of EBV-positive and -negative cell clones from a variety of EBV tumor lines. Since an isogenic system has been reported for only a few BL lines, with low frequency [11,16,43], such analytical subjects would benefit the progress of studies on EBV oncogenicity.

Concomitant with eradication of EBV, our dnEBNA1 inhibited the growth of the naturally occurring EBV-positive BL tumor cells in vitro and in vivo. Interestingly, this growth impairment was already evident in vitro 1 to 2 days after Adv inoculation, whereas EBV loss was usually recognizable 3 days after Adv inoculation. This implies that dnEBNA1 might interfere not only through eradication of viral episomes, but directly via a putative wtEBNA1 function implicated in activating the cell cycle [12,26,30], although this has yet to be confirmed [14,16,17,44]. Similar studies on tumor cells that have integrated EBV genomes will be necessary to test this possibility. A recent study by others utilizing similar EBNA1 mutants has suggested that EBV, and wtEBNA1 itself in particular, was involved in the survival/persistence in vitro and in vivo of virus-infected cells [45]. In the article, an apoptotic event was induced in some but not all cells expressing dnEBNA1. Consistent with the result, our data (unpublished) also showed that only a minor fraction (~ 25%) of dnEBNA1-delivered Akata-EC BL cells entered into early apoptosis, assessed by annexin V expression, before EBV genomes were eradicated, though this is not the case with Mutu I BL cells. These findings suggested again that dnEBNA1 would check the cell survival/growth, at least in BL cells, through apoptosis and another undefined mechanism(s) [45]. We are now further assessing the inhibitory effects of dnEBNA1 on the growth of various cell types, including EBV-carrying T or NK cells established spontaneously from lethal EBV-induced lymphoproliferative diseases [3,46].

Although the precise molecular mechanism by which our dnEBNA1 eliminates EBV from cells is not yet fully understood, several mechanisms are feasible based on the domain structure. The DNA binding/dimerization domain enables the dnEBNA1 molecules to dimerize, thereby competing against wtEBNA1 homodimers (functional form) for occupancy on the specific cis-acting element in oriP. In addition, dnEBNA1 could conceivably heterodimerize with wtEBNA1, as described in a recent report using a similar mutant [44]. This could result in a decrease in wtEBNA1 homodimers by depriving them of dimerization partners. The dnEBNA1–wtEBNA1 heterodimers (nonfunctional form) would also preclude binding of wtEBNA1 homodimers to oriP. In either case, dnEBNA1 is deemed to inhibit directly viral episome maintenance mediated by the interaction of the wtEBNA1 homodimer with oriP. Moreover, the inhibitory effects of dnEBNA1 against wtEBNA1 binding to oriP may abolish the enhancer activity of oriP for Cp and Wp, which decelerates wtEBNA1 mRNA transcription (and probably other EBNAs and LMP1/2B) in cells of Latency III [19,22,24,32,33,44]. Down regulation of wtEBNA1 synthesis would also occur in cells of Latency I or II because Qp-driven wtEBNA1 transcription is autorepressed via wtEBNA1 binding to negative regulatory elements for Qp (NRE-Qp) [25]. If dnEBNA1 homodimers

and/or dnEBNA1–wtEBNA1 heterodimers exist in abundance, they would bind to NRE-Qp, thus leading to down regulation of Qp activity. Such suppressive effects of dnEBNA1 on *de novo* wtEBNA1 synthesis via mediation of promoter regulation may also play an indirect role in inhibiting viral episome maintenance. Further investigation into this proposal is now being undertaken.

The molecular balance between dnEBNA1 and wtEBNA1 appears to be a critical factor in achieving efficient dominant-negative effects. This was seen here in the EBER1-ISH experiments, which showed that EBV-lost clones varied significantly, even in the same cell line, according to whether the introduced dnEBNA1 gene was driven by SVp or CMVp. For example, when NU-GC-3/rEBV cells were inoculated with Adv5-SV-DNE1 or with Adv5-CV-DNE1, at the same m.o.i. of 20, the incidence of EBER1-negative cells was significantly different: 69.3 ± 6.2% for SVp vs 88.6 ± 3.1% for CMVp ($P < 0.01$ by t test) 9 days postinoculation. The data indicate that there may be a minimum threshold of the stoichiometric dnEBNA1:wtEBNA1 ratio that can make the effects of dnEBNA1 overt, although this was not determined in the present study.

An epidemiological study estimates the annual incidence of EBV-associated human tumors worldwide to be approximately 500,000 [47]. These EBV-associated diseases are often uncontrollable by currently available treatments. A promising therapeutic approach against these diseases is adoptive immune transfer of EBV-specific cytotoxic T lymphocytes (CTL) [48,49], although several problems remain [50]. An alternative approach, based on evidence that the EBV genome, or the specific gene, is virtually implicated in the cellular acquisition of malignant phenotypes [1,7–18,43], involves single EBV gene- or EBV genome (machinery)-targeted remedial strategies, some of which are considered to have potential as treatments [51–55]. However, most EBV latent genes, other than EBNA1, are silenced in tumor cells [1,2,4,5,39,40,42,46] or are heterogeneously expressed, even in individual tumors [56–58], thus limiting clinical approaches that target these viral latent genes. Because of its wide applicability and selectivity, EBNA1-based or -targeted molecular therapy would be more suitable for clinical application [52,55,59].

Rigorous investigations have defined the CTL epitope-clustered location in EBNA1 as the C-terminal, DNA-binding/dimerization domain [60,61]. However, EBNA1-specific CD8+ CTL do not efficiently recognize target cells expressing the full-length EBNA1 protein [60]. This is due in part to the Gly2-Ala repeat domain, which inhibits MHC class I-restricted presentation of the epitopes of EBNA1 [62]. Our dnEBNA1 lacks the Gly2-Ala repeat domain, but still has the C-terminal, CTL epitope-rich region. This knowledge raises some concerns about the therapeutic use of dnEBNA1, for although transduction of dnEBNA1 may favorably potentiate EBNA1-specific

CTL recognition of virus-infected tumor cells, it may also expose normal cells to CTL. To avoid such disadvantages, tumor-specific transduction and/or expression of dnEBNA1 or intentional conservation of the Gly2-Ala repeats (preferably as a functionally minimal form) within the dnEBNA1 structure would be necessary.

MATERIALS AND METHODS

Cell lines. EBV-converted or -reinfected cell lines were established by infecting virus-negative cells with rEBV (Akata strain), which carries the *neo^r* as a selective marker [38]. In this study, each rEBV-positive line was denoted by the name of the EBV-negative parental cell line followed by "/rEBV" (Table 1), i.e., Akata⁻/rEBV [14], MT-2/rEBV [40], NU-GC-3/rEBV [15,39], and BJAB/rEBV [41]. Converted cell lines were maintained in RPMI 1640 culture medium containing 10% fetal calf serum and G418 (Sigma–Aldrich, Tokyo, Japan) at appropriate concentrations (0.5–1 mg/ml) for selection. In some experiments, G418 was removed from cultures during an observation period. Southern blot hybridization confirmed that all the converted cell lines harbored the rEBV genome in an episomal, not integrated, form (data not shown). Mutu I [42] (clone 79, kindly provided by Dr. J. Sample, St. Jude Children's Research Hospital, Memphis, TN, USA) and Akata-EC (early-cultured Akata) [17] were used as test cells of naturally EBV-infected BL cell lines. Hygromycin B (Wako Pure Chemical Industries, Ltd., Osaka, Japan) was used to grow cells selectively in dual gene transduction experiments (see below). The MRC-5 cell line was purchased from the American Type Culture Collection (Rockville, MD, USA). 293/DNE1 is a hygromycin-selected 293 cell clone that stably expresses the mtEBNA1 protein.

Plasmid construction. The mtEBNA1 structure was made according to the EBNA1 sequence of B95-8 EBV [63]. The mtEBNA1 consists of the following functional domains of wtEBNA1 (641 amino acids of the B95-8 strain): the nuclear localization signal (NLS; aa 379 to 386) and the C-terminal region spanning the DNA linking/dimerization domain to the acidic tail (aa 451 to 641) (Fig. 1) [22,32–34]. Briefly, a coding segment of the partial NLS (aa 382 to 386) connected to the C-terminal domain region (aa 451 to 641) was amplified by PCR using a cloned *Bam*HI-K of B95-8 EBV (pUC119-B95BamK) as the template. The mutagenized nucleotides ATC were introduced into the forward chimeric junction primer, in place of GAG in the native NLS (genomic coordinates 96807 to 96809 according to the new version of the B95-8 EBV sequence databases, GenBank Accession No. AJ507799), thereby generating a *Bgl*II recognition site useful for the next DNA recombination without amino acid substitution (relating to codons Arg³⁸² and Ser³⁸³). The reverse adaptor primer contained the artificial *Bal*I and *Eco*RI recognition sites (necessary for cloning) followed by sequences encompassing the 3′end of the acidic tail domain. An amplified product was cloned into the *Bgl*II–*Eco*RI site of the pIRES2-EGFP vector (BD Bioscience Clontech, Tokyo, Japan), resulting in pIRES2-EGFP/Bg-EI-ΔDNE1. A synthesized oligomer adaptor was then prepared, composed of coding sequences for the N-terminal part of mtEBNA1 (Met¹-Lys³⁷⁹-Arg³⁸⁰-Pro³⁸¹) with *Nhe*I- and *Bgl*II-compatible sites at its 5′and 3′ends, respectively. The adaptor was inserted into *Nhe*I–*Bgl*II site of pIRES2-EGFP/Bg-EI-ΔDNE1, yielding pIRES2-EGFP/DNE1. A 0.6-kb *Eco*RI fragment of pIRES2-EGFP/DNE1, corresponding to the expected entire structure of mtEBNA1, was cloned into SVp-driven vector, pSG5-neo, a modified pSG5 (Stratagene, La Jolla, CA, USA) into which the *neo^r* cassette had been inserted. The same 0.6-kb *Eco*RI fragment was cloned also into the CMVp-driven vector pcDNA3 (Invitrogen, Groningen, Netherlands), resulting in pSG5-neo/DNE1 and pcDNA3-DNE1, respectively. A wtEBNA1 expression plasmid, pSG5m-neo/AKE1, was constructed by ligating a 2.1-kb *Xho*II–*Bal*I fragment from a cloned *Bam*HI-K of Akata EBV strain [37] into the *Bam*HI–*Sma*I site of pSG5m-neo (pSG5-neo with additional cloning sites). Expression plasmids for EGFP (derived from pIRES2-EGFP) and *Escherichia coli* β-galactosidase (LacZ; derived from pSV-β-Gal; Promega, Madison, WI, USA) were also cloned into pSG5m-neo and pcDNA3.

Plasmids for IRES-mediated bicistronic expression of the mtEBNA1 gene and the *hyg*^r gene, as a positive selection marker, were also constructed for mtEBNA1-transduced cell sorting experiments (Fig. 4C). Briefly, the *hyg*^r–poly(A) segment of pCEP4 (Invitrogen) was PCR-amplified with primers to create *Eco*RV and *Xho*I recognition sequences at the 5′ and 3′ ends, respectively, and cloned into pBluescript II SK(−) (Stratagene), resulting in pBKN-HYG-pA. The *Eco*T22I (blunted)–*Bst*XI fragment from pIRES2-EGFP/DNE1, which contains CMVp-DNE1-IRES, was inserted into the *Sac*I (blunted)–*Bst*XI site of pBKN-HYG-pA, yielding the plasmid pCMV-DIH containing CMVp-DNE1-IRES-*hyg*^r-polyA. A plasmid containing SV40p-DNE1-IRES-*hyg*^r-polyA, pSG5-DIH, was also made by replacing CMVp of pCMV-DIH with SV40p. Plasmids for coexpression of lacZ and *hyg*^r (pCMV-LIH and pSG5-LIH) were constructed as controls.

The expression units of the plasmids described above (details will be provided upon request) were incorporated into Adv's as explained below.

Isolation and purification of Adv.
All Adv's used in this study were developed using the *in vitro* ligation method [35]. Adenovirus genome plasmids, termed pAdHM4 [35] and pAdHM36 [36], were used to construct the standard E1/E3-deleted Adv5 and its fiber-replaced variant (Adv5/35f), respectively. Prepared recombinant Adv genome plasmids were linearized with *Pac*I (New England Biolabs, Inc., Beverly, MA, USA) and then transfected into 293 cells. After plaque purification, Adv isolates were checked for the restriction pattern of viral DNA and expression of incorporated genes. Confirmed virus clones were expanded and purified by sequential ultracentrifugation, using CsCl step gradients, followed by dialysis [64]. Purified virus was aliquoted into small volumes and stored at −80°C until use. Titers of virus stock were determined by the standard plaque-forming end-point assay [64].

In this study, both SVp-driven and CMVp-driven expression units were constructed for each gene, e.g., pSG5-neo/DNE1 and pcDNA3-DNE1 (see above), and incorporated individually into Adv5 and Adv5/35f. Of the four kinds of Adv per gene, the most suitable for each cell line in terms of the highest gene transfer efficiency (Adv5 or Adv5/35f) and gene expression levels (SVp or CMVp). Adv's were designated "Adv type-driving promoter-incorporated gene." For example, Adv5 for SVp-driven mtEBNA1 and Adv5/35f for CMVp-driven LacZ were referred to as Adv5-SV-DNE1 and Adv5/35f-CV-LacZ, respectively. Adv's for IRES-mediated coexpression of mtEBNA1 (or LacZ) and *hyg*^r were referred to as Adv5 (or Adv5/35f)-SV (or CV)-DIH (or LIH) (Fig. 4C).

Adv infection and flow cytometric analysis.
Susceptibility of cell lines to Adv infection was examined by exposing cells to Adv5 (or Adv5/35f)-SV (or CV)-EGFP at various m.o.i. for 2 h at 37°C. After cultivation for 3 days, EGFP-positive cells were measured by flow cytometry (FACScan Cytometer, BD Bioscience Clontech) and compared with cells inoculated with each corresponding Adv type for LacZ expression at the same m.o.i. and with mock-inoculated cells as controls. Immediately before analysis, cells were stained with 2 μM 7-amino-actinomycin D (Sigma–Aldrich) to exclude nonviable cells.

Selection of Adv-infected cells.
Cells that had been successfully infected with Adv5-SV (or CV)-DIH (or LIH) were sorted from uninfected cells by hygromycin B-based positive selection (Fig. 4D). The optimal conditions for this short-term drug pulse were determined preliminarily for each cell line by strictly comparing Adv-DIH-inoculated cultures with Adv-LIH-inoculated cultures (selection procedures following Adv inoculation for Mutu I cells, as an example, are described under Results and in the legend to Fig. 4D). The resultant surviving cells after drug selection were then evaluated for EBV genome carriage (e.g., by *in situ* hybridization, see below). Using immunoblot analysis, it was confirmed that Adv5-SV (or CV)-DIH (or LIH) achieved the same levels of mtEBNA1 and LacZ protein expression as Adv5-SV (or CV)-DNE1 (or LacZ) did (data not shown).

Quantitative PCR.
The EBV genome was quantified by real-time PCR with the LightCycler system (Roche Diagnostics, Mannheim, Germany) using primers directed for a region within the LMP1 gene. The sequences

were LMP1-Pv4S, 5′-GTTGATCTCCTTTGGCTCCTC-3′ (genome coordinates 168358–168338, according to the new databases mentioned above), and LMP1-Pv4AS, 5′-GTGTCTGCCCTCGTTGG-3′ (168191–168207). Two specific hybridization probes were used: LMP1-v4PR/FL, 5′-TGATGAACAC-CACCACGATGACTCC-[fluorescein]-3′ (168287–168263), and LMP1-v4PR/LC, 5′-[LC-Red640]-TCCCGCACCCTCAACAAGCTAC-PO₄-3′ (168261–168240) (synthesized by Nihon Gene Research Labs, Inc., Sendai, Japan). Template DNA was extracted with a FlexiGene DNA Kit (Qiagen, Tokyo, Japan), treated with 20 μl of RNase A (10 μg/ml, type IA; Sigma–Aldrich), and predigested with *Eco*RI to minimize the viscosity of DNA solutions, thereby ensuring accuracy in the amount of DNA dispensed into capillaries. The reaction mixture was 20 μl in volume and consisted of 10 pmol of each primer, 4 pmol of each probe, 10 μl of QuantiTect Probe PCR Kit Master Mix (Qiagen), and 5 μl of the predigested DNA (50 ng) per reaction. The cycling protocol was as follows: preincubation at 94°C for 15 min followed by 40 cycles of denaturation at 94°C for 15 s, annealing at 60°C for 20 s, and extension at 72°C for 20 s. Data were gained according to the settings recommended by the manufacturer and analyzed with LightCycler software version 3.5. Serial 10-fold dilutions of a plasmid amplicon containing the LMP1 target sequence (2×10^4 to 2×10^1 copies per capillary) were used to generate a standard plot for calculation of EBV genome number. To calibrate the data and to check the integrity of DNA samples, the β-globin gene was quantified in parallel (information about primers/probes can be provided upon request). The Namalwa cell line [65], which carries two EBV genomes per cell, was used as a positive control for each LightCycler assay to check reproducibility.

Immunoblot.
The basic immunoblot procedures used have been described previously [46]. EBNA1 expression was examined with reference human serum (anti-EBNA1 titer, 1:1280) or EBNA1-monospecific rabbit immune serum (kindly provided by Dr. T. Tsurumi, Aichi Cancer Center, Nagoya, Japan) as the primary antibody. Protein bands were detected using the enhanced chemiluminescence system (Amersham Pharmacia). In some experiments, specific chemiluminescent signals were scanned by the ATTO LightCapture System Cool Saver software (Type AE-6962; ATTO Co. Ltd., Tokyo, Japan) and intensity was analyzed with a CS analyzer (ATTO). To evaluate the relative levels of wtEBNA1 protein expression, scanned values specific for wtEBNA1 were normalized to those of β-actin signals of the same samples probed with the AC-15 monoclonal antibody (Sigma–Aldrich) as an internal control.

Cell proliferation assay.
Viable cell kinetics were assessed by trypan blue dye exclusion or by production of water-soluble formazan in the sulfonated tetrazolium salt (WST-1) assay (Takara Biotech, Tokyo, Japan). The WST-1 assay was done in triplicate in 96-well plates, and an absorbance of 450 nm (A_{450}) was determined for each well, followed by subtracting the background absorbance (A_{600}) from each A_{450} measurement.

In situ hybridization.
To detect EBV genome-harboring cells, FISH was carried out according to the method reported previously [66]. Briefly, the cosmid pJB8, containing an *Eco*RI-A fragment (37 kb) of EBV DNA, was used to make a probe labeled with biotin-16-dUTP (Roche Diagnostics) by nick translation. Ten microliters of hybridization solution (Sigma–Aldrich) containing 20 ng of biotinylated probe was denatured at 70°C for 2 min and applied to preparations on glass slides, which were then incubated at 37°C overnight in a humidified chamber. The slides were washed twice for 10 min in 50% formamide in 2× standard saline citrate (SSC) (0.3 mM sodium chloride, 30 mM sodium citrate, pH 7.0) at 43°C, followed by two rinses in 2× SSC at 37°C. The hybridized probe was detected by incubation with fluorescein avidin D (Vector Laboratories, Burlingame, CA, USA), according to the procedure described previously [66]. The interphase nuclei were counterstained with propidium iodide (Sigma–Aldrich) and diamino-2-phenylindole (SERVA Feinbiochemica, Heidelberg, Germany). The slides were observed with a BX50 epifluorescence microscope (Olympus, Tokyo, Japan). Hybridization signals were captured with a cooled CCD camera and merged using a computer workstation equipped with the M-FISH system (Photometrics-Seki Technotron, Tokyo, Japan). EBER1-ISH was also carried out to assess the EBV persistence or loss in rEBV-converted cells, as previously described in detail [46].

ARTICLE

Animal experiments. All animal experiments were conducted according to the guidelines of the Animal Experiment Committee of Kochi Medical School. The therapeutic potential of mtEBNA1 was assessed by its ability to inhibit tumor growth/induction *in vivo* using a xenograft animal model. Mutu I BL cells (1×10^7) suspended in 200 μl of PBS, pH 7.2, were implanted subcutaneously in both hind flanks of 6- to 8-week-old SCID mice (female, FOX CHASE C.B-17/lcr-scid Jcl; CLEA, Tokyo, Japan). Twelve mice (i.e., 24 flanks) were used for this experiment. Once tumors had become unequivocally palpable (0.4–0.5 cm in diameter), mice received intratumoral injection of either Adv5-SV-DNE1 or Adv5-SV-LacZ as the control (10^8 pfu per dose) into each flank. Some mice received an injection of PBS in place of Adv5-SV-LacZ as a mock injection control. Adv5-SV-DNE1, Adv5-SV-LacZ, and PBS were injected into eight tumors each. In an additional experiment, Mutu I cells were preexposed to Adv5-SV-DNE1 or Adv5-SV-LacZ and on the next day 1×10^7 viable cells were likewise implanted in each flank of SCID mice (4 mice were tested). All mice were monitored for tumor growth/induction for up to 4 weeks after cell implantation and photographed and euthanized if the tumor exceeded 2 cm in dimension or the mouse was apparently ill. The resected tumors were weighed, and some of the tissues were examined histologically and screened for EBV.

Statistical analysis. Data of wtEBNA1 protein levels and cell growth kinetics were expressed as the relative ratio (or percentage) of scanned (or absorbance) values in cells inoculated with Adv's against those of mock-inoculated cells. The statistical method used was mainly two-way analysis of variance. In analyses of the effects of Adv's, the factors consisted of time after Adv inoculation and Adv type (Adv-DNE1 and Adv-LacZ) used, followed by the post hoc Tukey or Dunnett test. The t test and the Mann–Whitney U test were also used for some results. P values less than 0.05 were considered statistically significant.

ACKNOWLEDGMENTS

APPENDIX A. SUPPLEMENTARY DATA

Supplementary data associated with this article can be found, in the online version, at doi: 10.1016/j.ymthe.2004.12.017.

REFERENCES

1. Rickinson, A. B., and Kieff, E. (2001). Epstein–Barr virus. In *Fields Virology* (D. M. Knipe, P. M. Howley Eds.), 4th ed., Vol. 2, pp. 2575–2627. Lippincott, Philadelphia.
2. Pallesen, G., Hamilton-Dutoit, S. J., Rowe, M., and Young, L. S. (1991). Expression of Epstein–Barr virus latent gene products in tumour cells of Hodgkin's disease. *Lancet* 337: 320–322.
3. Harabuchi, Y., et al. (1990). Epstein–Barr virus in nasal T-cell lymphomas in patients with lethal midline granuloma. *Lancet* 335: 128–130.
4. Imai, S., et al. (1994). Gastric carcinoma: monoclonal epithelial malignant cells expressing Epstein–Barr virus latent infection protein. *Proc. Natl. Acad. Sci. USA* 91: 9131–9135.
5. Sugiura, M., et al. (1996). Transcriptional analysis of Epstein–Barr virus gene expression in EBV-positive gastric carcinoma: unique viral latency in the tumour cells. *Br. J. Cancer* 74: 625–631.
6. Jaffe, E. S., et al. (1996). Report of the Workshop on Nasal and Related Extranodal Angiocentric T/Natural Killer Cell Lymphomas: definitions, differential diagnosis, and epidemiology. *Am. J. Surg. Pathol.* 20: 103–111.
7. Kieff, E., and Rickinson, A. B. (2001). Epstein–Barr virus and its replication. In *Fields Virology* (D. M. Knipe, P. M. Howley Eds.), 4th ed., Vol. 2, pp. 2511–2573. Lippincott, Philadelphia.
8. Griffin, B. E., and Karran, L. (1984). Immortalization of monkey epithelial cells by specific fragments of Epstein–Barr virus DNA. *Nature* 309: 78–82.
9. Hammerschmidt, W., and Sugden, B. (1989). Genetic analysis of immortalizing functions of Epstein–Barr virus in human B lymphocytes. *Nature* 340: 393–397.
10. Wei, M. X., and Ooka, T. (1989). A transforming function of the BARF1 gene encoded by Epstein–Barr virus. *EMBO J.* 8: 2897–2903.
11. Shimizu, N., Tanabe-Tochikura, A., Kuroiwa, Y., and Takada, K. (1994). Isolation of Epstein–Barr virus (EBV)-negative cell clones from the EBV-positive Burkitt's lymphoma (BL) line Akata: malignant phenotypes of BL cells are dependent on EBV. *J. Virol.* 68: 6069–6073.
12. Wilson, J. B., Bell, J. L., and Levine, A. J. (1996). Expression of Epstein–Barr virus nuclear antigen-1 induces B cell neoplasia in transgenic mice. *EMBO J.* 15: 3117–3126.
13. Kulwichit, W., Edwards, R. H., Davenport, E. M., Baskar, J. F., Godfrey, V., and Raab-Traub, N. (1998). Expression of the Epstein–Barr virus latent membrane protein 1 induces B cell lymphoma in transgenic mice. *Proc. Natl. Acad. Sci. USA* 95: 11963–11968.
14. Komano, J., Maruo, S., Kurozumi, K., Oda, T., and Takada, K. (1999). Oncogenic role of Epstein–Barr virus-encoded RNAs in Burkitt's lymphoma cell line Akata. *J. Virol.* 73: 9827–9831.
15. Nishikawa, J., Imai, S., Oda, T., Kojima, T., Okita, K., and Takada, K. (1999). Epstein–Barr virus promotes epithelial cell growth in the absence of EBNA2 and LMP1 expression. *J. Virol.* 73: 1286–1292.
16. Kitagawa, N., et al. (2000). Epstein–Barr virus-encoded poly(A)$^-$ RNA supports Burkitt's lymphoma growth through interleukin-10 induction. *EMBO J.* 19: 6742–6750.
17. Maruo, S., Nanbo, A., and Takada, K. (2001). Replacement of the Epstein–Barr virus plasmid with the EBER plasmid in Burkitt's lymphoma cells. *J. Virol.* 75: 9977–9982.
18. Imai, S., Nishikawa, J., Kuroda, M., and Takada, K. (2001). Epstein–Barr virus infection of human epithelial cells. *Curr. Top. Microbiol. Immunol.* 258: 161–184.
19. Rogers, R. P., Woisetschlaeger, M., and Speck, S. H. (1990). Alternative splicing dictates translational start in Epstein–Barr virus transcripts. *EMBO J.* 9: 2273–2277.
20. Schaefer, B. C., Strominger, J. L., and Speck, S. H. (1995). Redefining the Epstein–Barr virus-encoded nuclear antigen EBNA-1 gene promoter and transcription initiation site in group I Burkitt lymphoma cell lines. *Proc. Natl. Acad. Sci. USA* 92: 10565–10569.
21. Yates, J. L., Warren, N., and Sugden, B. (1985). Stable replication of plasmids derived from Epstein–Barr virus in various mammalian cells. *Nature* 313: 812–815.
22. Leight, E. R., and Sugden, B. (2000). EBNA-1: a protein pivotal to latent infection by Epstein–Barr virus. *Rev. Med. Virol.* 10: 83–100.
23. Gahn, T. A., and Sugden, B. (1995). An EBNA-1-dependent enhancer acts from a distance of 10 kilobase pairs to increase expression of the Epstein–Barr virus LMP gene. *J. Virol.* 69: 2633–2636.
24. Puglielli, M. T., Woisetschlaeger, M., and Speck, S. H. (1996). OriP is essential for EBNA gene promoter activity in Epstein–Barr virus-immortalized lymphoblastoid cell lines. *J. Virol.* 70: 5758–5768.
25. Sample, J., Henson, E. B., and Sample, C. (1992). The Epstein–Barr virus nuclear protein 1 promoter active in type I latency is autoregulated. *J. Virol.* 66: 4654–4661.
26. Snudden, D. K., Hearing, J., Smith, P. R., Grasser, F. A., and Griffin, B. E. (1994). EBNA-1, the major nuclear antigen of Epstein–Barr virus, resembles 'RGG' RNA binding proteins. *EMBO J.* 13: 4840–4847.
27. Srinivas, S. K., and Sixbey, J. W. (1995). Epstein–Barr virus induction of recombinase-activating genes RAG1 and RAG2. *J. Virol.* 69: 8155–8158.
28. Kube, D., et al. (1999). Expression of Epstein–Barr virus nuclear antigen 1 is associated with enhanced expression of CD25 in the Hodgkin cell line L428. *J. Virol.* 73: 1630–1636.
29. Sugawara, Y., Makuuchi, M., Kato, N., Shimotohno, K., and Takada, K. (2000). Enhancement of hepatitis C virus replication by Epstein–Barr virus-encoded nuclear antigen 1. *EMBO J.* 18: 5755–5760.
30. Holowaty, M. N., et al. (2003). Protein profiling with Epstein–Barr nuclear antigen-1 reveals an interaction with the herpesvirus-associated ubiquitin-specific protease HAUSP/USP7. *J. Biol. Chem.* 278: 29987–29994.
31. Steigerwald-Mullen, P., Kurilla, M. G., and Braciale, T. J. (2000). Type 2 cytokines predominate in the human CD4(+) T-lymphocyte response to Epstein–Barr virus nuclear antigen 1. *J. Virol.* 74: 6748–6759.
32. Ceccarelli, D. F., and Frappier, L. (2000). Functional analyses of the EBNA1 origin DNA binding protein of Epstein–Barr virus. *J. Virol.* 74: 4939–4948.
33. Wu, H., Kapoor, P., and Frappier, L. (2002). Separation of the DNA replication, segregation, and transcriptional activation functions of Epstein–Barr nuclear antigen 1. *J. Virol.* 76: 2480–2490.
34. Kirchmaier, A. L., and Sugden, B. (1997). Dominant-negative inhibitors of EBNA-1 of Epstein–Barr virus. *J. Virol.* 71: 1766–1775.
35. Mizuguchi, H., and Kay, M. A. (1998). Efficient construction of a recombinant adenovirus vector by an improved in vitro ligation method. *Hum. Gene Ther.* 9: 2577–2583.
36. Mizuguchi, H., and Hayakawa, T. (2002). Adenovirus vectors containing chimeric type 5 and type 35 fiber proteins exhibit altered and expanded tropism and increase the size limit of foreign genes. *Gene* 285: 69–77.
37. Takada, K., et al. (1991). An Epstein–Barr virus-producer line Akata: establishment of the cell line and analysis of viral DNA. *Virus Genes* 5: 147–156.

38. Shimizu, N., Yoshiyama, H., and Takada, K. (1996). Clonal propagation of Epstein–Barr virus (EBV) recombinants in EBV-negative Akata cells. *J. Virol.* **70:** 7260–7263.

39. Imai, S., Nishikawa, J., and Takada, K. (1998). Cell-to-cell contact as an efficient mode of Epstein–Barr virus infection of diverse human epithelial cells. *J. Virol.* **72:** 4371–4378.

40. Yoshiyama, H., Shimizu, N., and Takada, K. (1995). Persistent Epstein–Barr virus infection in a human T-cell line: unique program of latent virus expression. *EMBO J.* **14:** 3706–3711.

41. Kanamori, M., *et al.* (2004). Epstein–Barr virus nuclear antigen leader protein induces expression of thymus and activation-regulated chemokine in B cells. *J. Virol.* **78:** 3984–3993.

42. Gregory, C. D., Rowe, M., and Rickinson, A. B. (1990). Different Epstein–Barr virus–B cell interactions in phenotypically distinct clones of a Burkitt's lymphoma cell line. *J. Gen. Virol.* **71:** 1481–1495.

43. Chodosh, J., Holder, V. P., Gan, Y. J., Belgaumi, A., Sample, J., and Sixbey, J. W. (1998). Eradication of latent Epstein–Barr virus by hydroxyurea alters the growth-transformed cell phenotype. *J. Infect. Dis.* **177:** 1194–1201.

44. Kang, M. S., Hung, S. C., and Kieff, E. (2001). Epstein–Barr virus nuclear antigen 1 activates transcription from episomal but not integrated DNA and does not alter lymphocyte growth. *Proc. Natl. Acad. Sci. USA* **98:** 15233–15238.

45. Kennedy, G., Komano, J., and Sugden, B. (2003). Epstein–Barr virus provides a survival factor to Burkitt's lymphomas. *Proc. Natl. Acad. Sci. USA* **100:** 14269–14274.

46. Imai, S., *et al.* (1996). Epstein–Barr virus (EBV)-carrying and -expressing T-cell lines established from severe chronic active EBV infection. *Blood* **87:** 1446–1457.

47. Levin, L. I., and Levine, P. H. (1998). The epidemiology of Epstein–Barr virus-associated human cancer. *Gann Monogr. Cancer Res.* **45:** 51–74.

48. Heslop, H. E., *et al.* (1996). Long-term restoration of immunity against Epstein–Barr virus infection by adoptive transfer of gene-modified virus-specific T lymphocytes. *Nat. Med.* **2:** 551–555.

49. Gottschalk, S., *et al.* (2003). Generating CTLs against the subdominant Epstein–Barr virus LMP1 antigen for the adoptive immunotherapy of EBV-associated malignancies. *Blood* **101:** 1905–1912.

50. Gottschalk, S., *et al.* (2001). An Epstein–Barr virus deletion mutant associated with fatal lymphoproliferative disease unresponsive to therapy with virus-specific CTLs. *Blood* **97:** 835–843.

51. Banerjee, S., Livanos, E., and Vos, J. M. H. (1995). Therapeutic gene delivery in human B-lymphoblastoid cells by engineered non-transforming infectious Epstein–Barr virus. *Nat. Med.* **1:** 1303–1308.

52. Judde, J. G., Spangler, G., Magrath, I., and Bhatia, K. (1996). Use of Epstein–Barr virus nuclear antigen-1 in targeted therapy of EBV-associated neoplasia. *Hum. Gene Ther.* **7:** 647–653.

53. Franken, M., Estabrooks, A., Cavacini, L., Sherburne, B., Wang, F., and Scadden, D. T. (1996). Epstein–Barr virus-driven gene therapy for EBV-related lymphomas. *Nat. Med.* **2:** 1379–1382.

54. Westphal, E. M., Mauser, A., Swenson, J., Davis, M. G., Talarico, C. L., and Kenney, S. C. (1999). Induction of lytic Epstein–Barr virus (EBV) infection in EBV-associated malignancies using adenovirus vectors in vitro and in vivo. *Cancer Res.* **59:** 1485–1491.

55. Li, J. H., *et al.* (2002). Tumor-targeted gene therapy for nasopharyngeal carcinoma. *Cancer Res.* **62:** 171–178.

56. Niedobitek, G., *et al.* (1995). Heterogeneous expression of Epstein–Barr virus latent proteins in endemic Burkitt's lymphoma. *Blood* **86:** 659–665.

57. Tao, Q., Robertson, K. D., Manns, A., Hildesheim, A., and Ambinder, R. F. (1998). Epstein–Barr virus (EBV) in endemic Burkitt's lymphoma: molecular analysis of primary tumor tissue. *Blood* **91:** 1373–1381.

58. Xue, S. A., *et al.* (2002). Promiscuous expression of Epstein–Barr virus genes in Burkitt's lymphoma from the central African country Malawi. *Int. J. Cancer* **99:** 635–643.

59. Roth, G., Curiel, T., and Lacy, J. (1994). Epstein–Barr viral nuclear antigen 1 antisense oligodeoxynucleotide inhibits proliferation of Epstein–Barr virus-immortalized B cells. *Blood* **84:** 582–587.

60. Blake, N., *et al.* (1997). Human CD8$^+$ T cell responses to EBV EBNA1: HLA class I presentation of the (Gly-Ala)-containing protein requires exogenous processing. *Immunity* **7:** 791–802.

61. Paludan, C., *et al.* (2002). Epstein–Barr nuclear antigen 1-specific CD4(+) Th1 cells kill Burkitt's lymphoma cells. *J. Immunol.* **169:** 1593–1603.

62. Levitskaya, J., Shapiro, A., Leonchiks, A., Ciechanover, A., and Masucci, M. G. (1997). Inhibition of ubiquitin/proteasome-dependent protein degradation by the Gly-Ala repeat domain of the Epstein–Barr virus nuclear antigen 1. *Proc. Natl. Acad. Sci. USA* **94:** 12616–12620.

63. Baer, R., *et al.* (1984). DNA sequence and expression of the B95-8 Epstein–Barr virus genome. *Nature* **310:** 207–211.

64. Kanegae, Y., Makimura, M., and Saito, I. (1994). A simple and efficient method for purification of infectious recombinant adenovirus. *Jpn. J. Med. Sci. Biol.* **47:** 157–166.

65. Prichett, R., Pedersen, M., and Kieff, E. (1976). Complexity of EBV homologous DNA in continuous lymphoblastoid cell lines. *Virology* **74:** 227–231.

66. Taguchi, T., *et al.* (1993). Chromosomal localization of the OX44 (CD53) leukocyte antigen gene in man and rodents. *Cytogenet. Cell Genet.* **64:** 217–221.

RNA interference of PPARγ using fiber-modified adenovirus vector efficiently suppresses preadipocyte-to-adipocyte differentiation in 3T3-L1 cells

Tetsuji Hosono[a], Hiroyuki Mizuguchi[b,*], Kazufumi Katayama[c], Naoya Koizumi[b,d], Kenji Kawabata[b], Teruhide Yamaguchi[a], Shinsaku Nakagawa[c], Yoshiteru Watanabe[d], Tadanori Mayumi[e], Takao Hayakawa[f]

[a]Division of Cellular and Gene Therapy Products, National Institute of Health Sciences, Tokyo 158-8501, Japan
[b]Project III, National Institute of Health Sciences, Osaka Branch, Fundamental Research Laboratories for Development of Medicine, Asagi 7-6-8, Saito, Ibaraki, Osaka 567-0085, Japan
[c]Department of Biopharmaceutics, Graduate School of Pharmaceutical Sciences, Osaka University, Osaka 565-0871, Japan
[d]Department of Pharmaceutics and Biopharmaceutics, Showa Pharmaceutical University, Tokyo 194-8543, Japan
[e]Faculty of Pharmaceutical Sciences, Kobe Gakuin University, Hyogo 651-2180, Japan
[f]National Institute of Health Sciences, Tokyo 158-8501, Japan

Abstract

The peroxisome proliferator-activated receptor (PPAR) γ is regarded as a "master regulator" of adipocyte differentiation and is abundantly expressed in adipose. To understand the biological role of PPARγ in adipose, RNA interference (RNAi) of PPARγ should be a powerful tool. 3T3-L1 cell line serves an excellent model to investigate the mechanism of preadipocyte-to-adipocyte differentiation. However, this cell line is difficult to transfect by plasmid vectors and viral vectors. We optimized the transduction of both 3T3-L1 preadipocytes and adipocytes by means of fiber-modified adenovirus (Ad) vectors. Among the various vectors tested, polylysine modification of the C-terminal of the fiber knob most markedly improved the transduction efficiency in both 3T3-L1 preadipocytes and adipocytes. Then, we examined whether fiber-modified Ad vectors with polylysine peptides expressing the small interfering RNA (siRNA) for PPARγ inhibit the differentiation of 3T3-L1 preadipocytes into adipocytes. Oil red O staining and measurement of glycerol-3-phosphate dehydrogenase (GPDH) activity indicated that the vectors effectively suppressed the differentiation of 3T3-L1 preadipocytes to adipocytes. These results suggested that the combination of fiber-modified Ad vectors containing polylysine peptides and RNAi is an effective tool for the study of the biological and physiological mechanism of adipogenesis in adiposity and diabetes using 3T3-L1 models. Ad vector-mediated RNAi for PPARγ should also be useful to clarify the biological role of the PPARγ pathway in various tissues in addition to adipose and for therapeutic application to a variety of diseases, including adiposity and diabetes.
© 2005 Elsevier B.V. All rights reserved.

Keywords: Adenovirus vector; PPARγ; RNA interference; Adipocyte

1. Introduction

An understanding of the biological and physiological mechanism of adipogenesis is essential for an improved understanding of adiposity and diabetes. The expression of many transcription factors and adipocyte-specific genes, including CCAAT enhancer binding proteins (C/EBP) and

adipocyte differentiation and determination factor 1/sterol regulatory element binding protein 1 (ADD-1/SREBP-1), is programmatically regulated in the process of adipogenesis (Gregoire et al., 1998; Ntambi and Young-Cheul, 2000). Among them, the peroxisome proliferator-activated receptor (PPAR) γ is regarded as a "master regulator" of adipocyte differentiation and is abundantly expressed in adipose (Tontonoz et al., 1994a,b; Vidal-Puig et al., 1997; Wu et al., 1998; Kubota et al., 1999; Berger and Moller, 2002). PPARγ is a member of the nuclear receptor superfamily and induces transcriptional activation by heterodimerization with the retinoic acid-like receptor (RXR) (Tontonoz et al., 1994a; Berger and Moller, 2002).

Adipocytes are thought to be derived from mesenchymal stem cells, and cell culture models using preadipocyte 3T3-L1 cell lines are extensively used to study preadipocyte-to-adipocyte differentiation (Ntambi and Young-Cheul, 2000). Treatment of 3T3-L1 adipocytes with agonists for PPARγ including thiazolidinediones (TZD), potent insulin sensitizing agents, induces preadipocyte-to-adipocyte differentiation. To understand the factors and mechanisms involved in the process of adipogenesis, studies of loss of function via knock-out/knock-down of target gene expression or gain of function via overexpression are among the most powerful methods. 3T3-L1 cells, however, are not efficiently transfectable. Viral vector-mediated transduction might improve their efficiency.

Among the viral vectors, adenovirus (Ad) vectors have been extensively used to deliver foreign genes to a variety of cell types and tissues both in vitro and in vivo. They can be easily grown to high titer and can efficiently transfer genes into both dividing and non-dividing cells. The efficiency of Ad vector-mediated transduction into 3T3-L1 cells, however, is quite low due to the scarcity of the primary receptor, the coxsackievirus and adenovirus receptor (CAR) (Orlicky et al., 2001). To overcome CAR-dependent transduction, fiber-modified Ad vectors have been developed (Krasnykh et al., 1996; Wickham et al., 1997; Dmitriev et al., 1998; Shayakhmetov et al., 2000; Havenga et al., 2001; Mizuguchi et al., 2001; Mizuguchi and Hayakawa, 2002; Koizumi et al., 2003), containing RGD peptides in the HI loop of the fiber knob, polylysine peptides in the C-terminal end of the fiber knob, or fiber proteins derived from subgroup B Ads such as Ad type 3, -11, or -35. These vectors are infected via αv integrin, heparan sulfates, or CD46 (or CD80 or CD86) on the cellular surface, respectively (Wickham et al., 1997; Dmitriev et al., 1998; Mizuguchi et al., 2001; Gaggar et al., 2003; Segerman et al., 2003; Short et al., 2004).

For studies of loss of function via knockdown of target gene expression, RNA interference (RNAi) has been shown to have great promise for both basic research and therapeutic use. RNAi mediates the sequence-specific suppression of gene expression in a wide variety of eukaryotes by double-stranded RNA homologies to the target gene (McManus and Sharp, 2002). In mammalian cells, small interfering RNA (siRNA), a 19- to 29-nt RNA, leads to the inhibition of target gene expression in a sequence-specific manner

(Elbashir et al., 2001). Vector-based siRNA systems, including Ad vectors, have also been developed using RNA polymerase III promoters, such as the U6 promoter or the H1 promoter, to express siRNA (Brummelkamp et al., 2002; Miyagishi and Taira, 2002; Paul et al., 2002; Sui et al., 2002; Yu et al., 2002; Shen et al., 2003; Zhao et al., 2003; Hosono et al., 2004).

In the present study, we established an optimal fiber-modified Ad vector for transduction of 3T3-L1 preadipo-cytes and adipocytes and demonstrated that the fiber-modified Ad vector expressing short hairpin RNA (shRNA) against PPARγ efficiently suppressed the differentiation of preadipocytes into adipocytes in 3T3-L1 cells.

2. Materials and methods

2.1. Cells

293 cells and 3T3-L1 cells (clonal subline of the mouse 3T3 that accumulate large amounts of triglyceride fat when the cells are in the resting state; Human Science Research Resources Bank, Japan, JCRB9014) were cultured with Dulbecco's Modified Eagle's Medium supplemented with 10% fetal calf serum (FCS). NIH3T3 cells were cultured with minimum essential medium supplemented with 10% FCS.

2.2. Construction of stable CAR-expressing NIH3T3 cells

Mouse liver total RNA was isolated using ISOGEN reagent (Nippon Gene, Tokyo, Japan) according to the manufacturer's instructions. Mouse liver cDNA was obtained from reverse transcription (RT) product for mouse liver total RNA using a SuperScript First-Strand Synthesis System for RT-PCR (Invitrogen Life Technologies, Carls-bad, CA, USA) according to the manufacturer's instructions. Mouse CAR cDNA was amplified from mouse liver cDNA using the following primers: 5′-accatggcgcgcc-tactgtgct-3′ and 5′-ttcagtagtccttcatatttat -3′. The amplified polymerase chain reaction (PCR) product was inserted into the TA cloning vector pGEM-T Easy (Promega Corp., Madison, WI, USA) to generate pGEM-T-mCAR. CAR-expressing plasmid pCMV-mCAR was constructed by ligation of the EcoRI site of pcDNA3 (Invitrogen Life Technologies) with the EcoRI fragment of pGEM-T-mCAR, and was transfected into NIH3T3 cells by SuperFect transfection reagent (Qiagen, Inc., Valencia, CA, USA). The stable CAR-expressing cells, NIH3T3-CAR, were obtained by geneticin (G418) selection.

2.3. Plasmid and virus

pHMCA-LacZ1 contains a β-actin promoter/CMV enhancer with a β-actin intron, which was kindly provided by Dr. J. Miyazaki (Osaka University, Osaka, Japan) (Niwa et al., 1991), an Escherichia coli β-galactosidase (LacZ)

gene derived from pCMVβ (Clontech, Palo Alto, CA, USA), and a bovine growth hormone polyadenylation signal, flanked by *I-Ceu*I and *PI-Sce*I sites.

pHM5-H1-PPARγ was constructed by insertion of the oligonucleotides (5′-gatccccgtctgctgatctgcgagccttcaagagaggctcgcagatcagcagacttttggaaat-3′ and 5′-ctagatttccaaaaagtctgctgatctgcgagcctctcttgaaggctcgcagatcagcagacggg-3′) (Katayama et al., 2004) (loop sequences were underlined) into the *Bgl*II and *Xba*I sites of pHM5-H1 (Hosono et al., 2004), which is designed to express shRNA upon the insertion of an appropriate sequence into the *Bgl*II/*Xba*I site. pHM5-H1-Scramble was constructed by insertion of the oligonucleotides (5′-gatccccacgctgagtacttcgaaatttcaagagaatttcgaagtactcagcgtttttggaaat-3′ and 5′-ctagatttccaaaaaacgctgagtacttcgaaattctcttgaaatttcgaagtactcagcgggg-3′) (loop sequences were underlined) into the *Bgl*II and *Xba*I sites of pHM5-H1. The sequence was verified on a DNA sequencer (ABI PRISM 310, Applied Biosystems, Foster City, CA, USA).

Ad vectors expressing LacZ or siRNA were constructed by an improved in vitro ligation method (Mizuguchi and Kay, 1998; Mizuguchi and Kay, 1999). Briefly, pHMCA-LacZ1 was digested with *I-Ceu*I and *PI-Sce*I, and then ligated with *I-Ceu*I/*PI-Sce*I-digested pAdHM4 (Mizuguchi and Kay, 1998), pAdHM15-RGD (Mizuguchi et al., 2001), pAdHM41-K7(C) (Koizumi et al., 2003), or pAdHM34 (Mizuguchi and Hayakawa, 2002), resulting in pAdHM4-CALacZ1, pAdHM15-RGD-CALacZ1, pAdHM41-K7-CALacZ1, or pAdHM34-CALacZ1, respectively. pAdHM41-K7-H1, pAdHM41-K7-H1-PPARγ, and pAdHM41-K7-Scramble were constructed by the ligation of *I-Ceu*I/*PI-Sce*I-digested pHM5-H1, pHM5-H1-PPARγ, or pHM5-H1-Scramble, respectively, with *I-Ceu*I/*PI-Sce*I-digested pAdHM41-K7(C).

To generate the virus (Ad-CALacZ, AdRGD-CALacZ, AdF35-CALacZ, AdK7-CALacZ, AdK7-H1, AdK7-H1-PPARγ, AdK7-H1-Scramble), *Pac*I-digested Ad vector plasmids (pAdHM4-CALacZ1, pAdHM15-RGD-CALacZ1, pAdHM34-CALacZ1, pAdHM41-K7-CALacZ1, pAdHM41-K7-H1, pAdHM41-K7-H1-PPARγ, and pAdHM41-K7-Scramble, respectively) were transfected into 293 cells plated in a 60-mm dish with SuperFect (Qiagen, Inc.) according to the manufacturer's instructions. Viruses were prepared as described previously (Mizuguchi and Kay, 1998). AdK7-Null contains no transgene in the E1 deletion region. The virus was purified by $CsCl_2$ gradient centrifugation, dialyzed with the solution containing 10 mM Tris (pH 7.5), 1 mM $MgCl_2$ and 10% glycerol, and stored in aliquots at -70 °C. The determination of virus particle titer was accomplished spectrophotometrically by the method of Maizel et al. (1968).

2.4. X-gal staining

In the case of 3T3-L1 preadipocytes, 3T3-L1 cells (1×10^5 cells) were seeded into a 12-well plates. On the following day, they were transduced with Ad-CALacZ, AdRGD-CALacZ, AdF35-CALacZ, or AdK7-CALacZ (3000 or 10,000 vector particles (VP)/cell) for 1.5 h. Forty-eight hours later, LacZ production in the cells was determined by X-gal (5-bromo-4-chloro-3-indolyl-β-D-galactopyranoside) staining.

In the case of 3T3-L1 adipocytes, 3T3-L1 cells were differentiated as described in the next section. After 6 days in culture with differentiation medium, the cells were transduced with each Ad vector (3000 or 10,000 vector particles (VP)/cell) for 1.5 h. Forty-eight hours later, LacZ production in the cells was determined by X-gal staining.

2.5. Adipocyte differentiation

Induction of adipocyte differentiation was performed as previously described (Tontonoz et al., 1994a). Two days after confluence (day 0), the medium was replaced with differentiation medium containing pioglitazone (CALBIOCHEM, San Diego, CA, USA) (3 μM), insulin (Sigma, Saint Louis, MO, USA) (150 nM), dexamethasone (Sigma) (1 μM) and 3-isobutyl-1-methylxanthine (Sigma) (100 μM), which was changed every 3 days thereafter until analysis.

Differentiation of 3T3-L1 preadipocytes to adipocytes was monitored by measurement of intracellular lipid accumulation using Oil red O staining and glycerol-3-phosphate dehydrogenase (GPDH) activity on day 9. The cells were fixed for 2 h with 10% formaldehyde in isotonic phosphate buffer and then washed with distilled water. The cells were then stained with complete immersion in a

Table 1
Adenovirus vectors used in this study

Name	Fiber type	Gene of interest
Ad-CALacZ	type 5 fiber	CA promoter+LacZ
AdRGD-CALacZ	RGD peptide in the HI-loop of the fiber knob	CA promoter+LacZ
AdK7-CALacZ	polylysine peptide in the C-terminal of the fiber knob	CA promoter+LacZ
AdF35-CALacZ	chimeric type 5 fiber tail and type 35 fiber knob and shaft	CA promoter+LacZ
AdK7-H1	polylysine peptide in the C-terminal of the fiber knob	H1 promoter
AdK7-H1-PPARγ	polylysine peptide in the C-terminal of the fiber knob	H1 promoter+shRNA for PPARγ
AdK7-H1-Scramble	polylysine peptide in the C-terminal of the fiber knob	H1 promoter+shRNA for Scramble
AdK7-Null	polylysine peptide in the C-terminal of the fiber knob	none

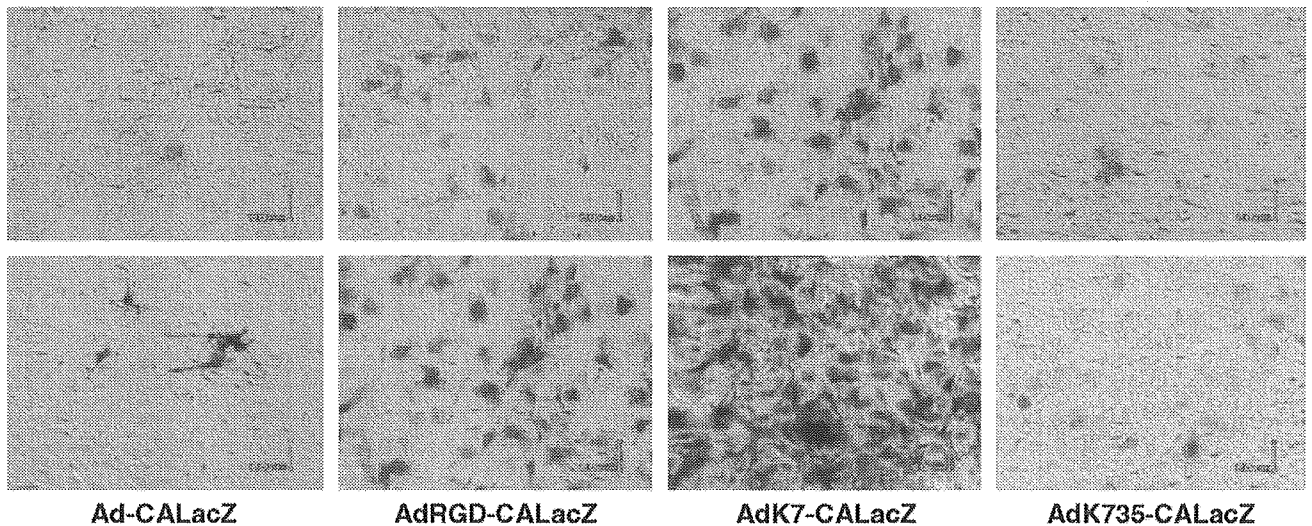CA promoter: β-actin promoter/CMV enhancer with β-actin intron.

working solution (0.3%) of Oil red O for 4 h. Excess dye was removed by exhaustive washing with water. The GPDH activity was measured using a GPDH assay kit (Hokudo, Hokkaido, Japan).

2.6. Reverse transcription–polymerase chain reaction for CAR mRNAs

Total RNA was isolated using ISOGEN reagent according to the manufacturer's instructions. RT was carried out using a SuperScript First-Strand Synthesis System for reverse transcription–polymerase chain reaction (RT-PCR) according to the manufacturer's instructions.

PCR amplification of the mouse CAR and GAPDH was performed in 50 μl of a solution containing 1 μl of RT products, 1 U TaKaRa Ex Taq HS and attached reagents (TaKaRa, Shiga, Japan). The sequences of the primer for PCR are as follows: CAR: forward, 5′-aattcctgctgaccgttctt-3′; reverse, 5′-tttctgccagccatggcgta-3′; GAPDH: forward, 5′-accacagtccatgccatcac-3′; reverse, 5′-tccaccaccctgttgctgta-3′. The following parameters were used: CAR: 20 s at 94 °C, 10 s at 60 °C, and 60 s at 72 °C for 35 cycles; GAPDH: 20 s at 94 °C, 10 s at 60 °C, and 60 s at 72 °C for 25 cycles. The PCR products were electrophoresed in 2.0% agarose gel. The sequence of the PCR products was confirmed by direct sequencing.
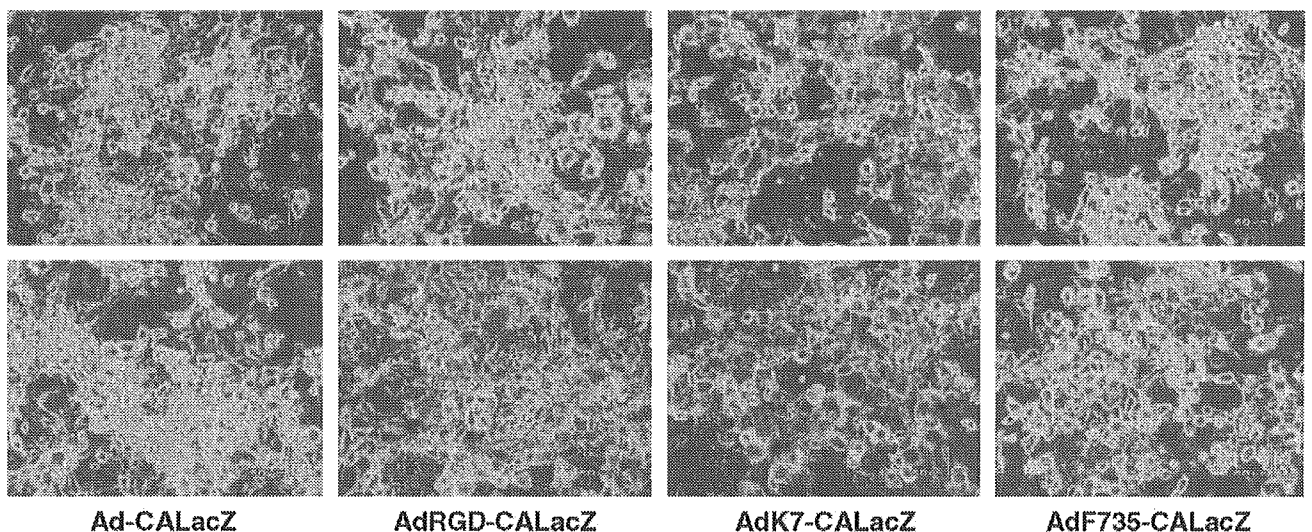
[A] Preadipocyte

| Ad-CALacZ | AdRGD-CALacZ | AdK7-CALacZ | AdK735-CALacZ |

[B] Adipocyte

| Ad-CALacZ | AdRGD-CALacZ | AdK7-CALacZ | AdF735-CALacZ |

Fig. 1. Comparison of the transduction efficiency of various types of fiber-modified Ad vector into 3T3-L1 preadipocytes and adipocytes. 3T3-L1 preadipocytes (A) and adipocytes (B), which were cultured in differentiation medium containing pioglitazone, insulin, dexamethasone and 3-isobutyl-1-methylxanthine for 6 days, were transduced with Ad-CALacZ, AdRGD-CALacZ, AdK7-CALacZ or AdF35-CALacZ (3000 or 10,000 VP/cells) for 1.5 h. After 48 h in culture, LacZ expression was determined by X-gal staining.

2.7. Western blotting for PPARγ proteins

The cell extracts were prepared in lysis buffer (25 mM Tris [pH 7.5], 1% Triton X-100, 0.5% sodium deoxycholate, 5 mM EDTA, 150 mM NaCl) containing a cocktail of protease inhibitors (Sigma). The protein content was measured with a Bio-Rad assay kit (Bio-Rad, Hercules, CA, USA) using bovine serum albumin as the standard. The protein samples (10 μg) were electrophoresed on 12.5% SDS–polyacrylamide gels under reducing conditions, followed by electrotransfer to Immobilon-P membranes (Millipore, Bedford, MA, USA). After blocking in Block Ace (Dainippon Pharmaceuticals, Osaka, Japan), the filters were incubated with antibodies against PPARγ (Santa Cruz Biotechnology, Inc., Santa Cruz, CA, USA) and GAPDH (Trevigen, Gaithersburg, MD, USA), followed by incubation in the presence of peroxidase-labeled horse anti-mouse IgG antibody (Cell Signaling Technology, Inc., Beverly, MA, USA) or peroxidase-labeled goat anti-rabbit IgG antibody (Cell Signaling Technology, Inc.). The filters were developed using chemiluminescence (ECL Western blotting detection system; Amersham Biosciences, Piscataway, NJ, USA). The signals were read using a LAS-3000 (FUJI-FILM, Tokyo, Japan), and quantified by Image Gauge Software (FUJIFILM).

3. Results

3.1. Optimization of fiber-modified Ad vectors for the transduction of 3T3-L1 adipocytes and preadipocytes

The Ad vector is known to transduce 3T3-L1 preadipocytes with very low efficiency (Orlicky et al., 2001; Orlicky and Schaack, 2001; Ross et al., 2003). Therefore, we first optimized the transduction of 3T3-L1 adipocytes as well as preadipocytes by means of fiber-modified Ad vectors, which exhibit different tropism with the conventional Ad vector.
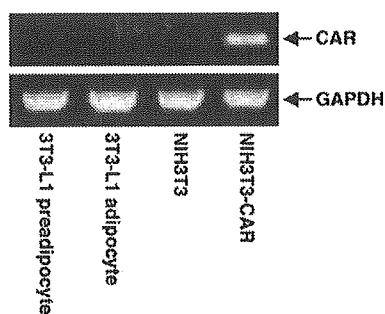

Fig. 2. RT-PCR analysis of CAR mRNA expression in 3T3-L1 preadipocytes and adipocytes. Total RNA was isolated from 3T3-L1 preadipocytes and adipocytes differentiated for 6 days, and RT-PCR analysis was performed as described in Materials and methods. NIH3T3 and NIH3T3-CAR cells were also analyzed as a negative and positive control of CAR mRNA expression, respectively.
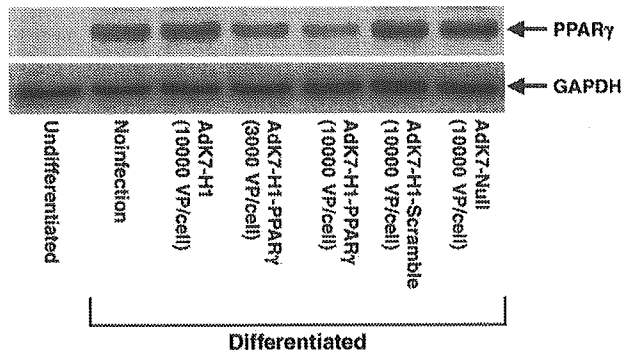

Fig. 3. Suppression of PPARγ expression in 3T3-L1 cells transduced with AdK7-H1-PPARγ. 3T3-L1 preadipocytes were transduced with each Ad vector for 1.5 h. On the following day, the cells reached confluence. From 3 days after Ad treatment, the cells were cultured with differentiation medium containing pioglitazone, insulin, dexamethasone and 3-isobutyl-1-methylxanthine for 4 days. Proteins were then extracted from the cells, and the levels of PPARγ expression were examined by Western blotting. The GAPDH bands served as an internal control for equal total protein loading.

The 3T3-L1 preadipocytes were infected with LacZ-expressing Ad vectors containing modified fiber proteins (Ad-CALacZ, AdRGD-CALacZ, AdF35-CALacZ and AdK7-CALacZ) (Table 1 and Fig. 1A). Ad-CALacZ contains the wild-type fiber, AdRGD-CALacZ contains an RGD peptide motif in the HI-loop of the fiber knob, AdK7-CALacZ contains a polylysine peptide in the C-terminal of the fiber knob, and AdF35-CALacZ contains a fiber protein derived from Ad type 5 fiber tail and Ad type 35 fiber knob and shaft. As shown previously (Orlicky et al., 2001; Orlicky and Schaack, 2001; Ross et al., 2003), Ad-CALacZ was inefficient for transduction of 3T3-L1 preadipocytes. AdK7-CALacZ was the most effective in transducing the LacZ genes. Nearly 100% of 3T3-L1 preadipocytes were transduced by AdK7-CALacZ at 10,000 vector particles (VP)/cell. AdRGD-CALacZ mediated higher levels of LacZ expression than Ad-CALacZ but lower levels than AdK7-CALacZ, while AdF35-CALacZ was ineffective.

We then examined the transduction efficiency of 3T3-L1 adipocytes using various types of Ad vectors. 3T3-L1 preadipocytes differentiate into mature, lipid droplet-containing adipocytes when stimulated with an appropriate hormonal cocktail containing insulin, dexamethasone and 3-isobutyl-1-methylxanthine. Pioglitazone, the ligand of PPARγ, enhances adipocyte differentiation of 3T3-L1 cells. 3T3-L1 preadipocytes were cultured with a differentiation medium containing pioglitazone for 6 days and then transduced with Ad vectors (Fig. 1B). Under the differentiated conditions, AdK7-CALacZ showed high transduction efficiency (67% LacZ-positive cells), although its efficiency was slightly lower than that in 3T3-L1 preadipocytes. AdRGD-CALacZ also showed high transduction efficiency (59% LacZ-positive cells). Ad-CALacZ and AdF35-CALacZ were ineffective. No cytotoxicity or other negative effects on cell function were observed in either 3T3-L1 preadipocytes or adipocytes.

To determine why the wild-type Ad vector exhibited inefficient transduction of 3T3-L1 preadipocytes and adipocytes, we examined the expression of CAR, a primary Ad receptor, in 3T3-L1 preadipocytes and adipocytes by RT-PCR analysis (Fig. 2). NIH3T3 and NIH3T3-CAR cells, which are transfectants of the mouse CAR gene, were used as a negative and positive control, respectively. The results showed that CAR mRNA was not present in either 3T3-L1 preadipocytes or adipocytes, suggesting that Ad vectors containing wild-type fiber did not mediate transduction probably due to little expression of CAR. From these

results, we concluded that fiber-modification with K7 peptides improved the efficiency of Ad transduction into both 3T3-L1 preadipocytes and adipocytes.

3.2. Suppression of the expression levels of PPARγ in 3T3-L1

Next, we constructed AdK7-H1-PPARγ, which expresses siRNA for PPARγ with K7 peptides-modified fiber knob, and examined whether AdK7-H1-PPARγ inhibited the differentiation of 3T3-L1 preadipocytes into adipocytes. The target
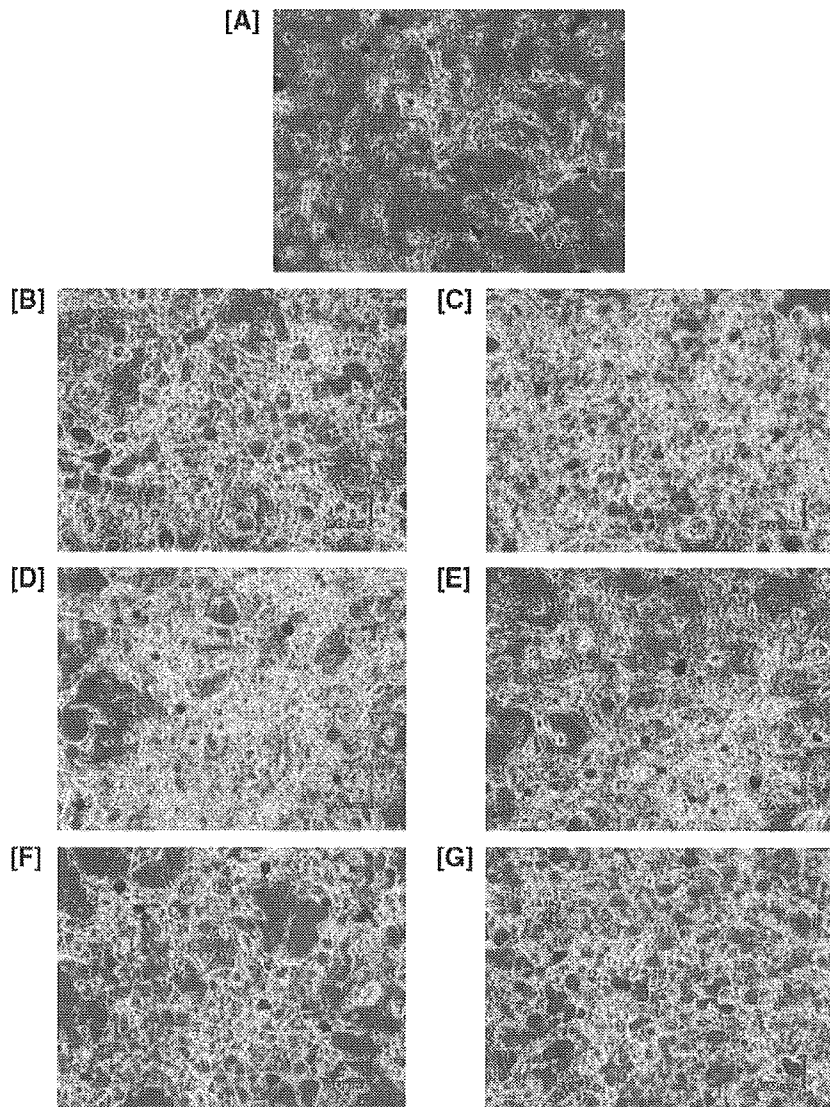

Fig. 4. Suppression of preadipocyte-to-adipocyte differentiation by transduction with AdK7-H1-PPARγ. 3T3-L1 preadipocytes were transduced with each Ad vector for 1.5 h. On the following day, the cells reached confluence. From 3 days after Ad treatment, the cells were cultured with differentiation medium containing pioglitazone, insulin, dexamethasone and 3-isobutyl-1-methylxanthine for 9 days. Then, the intracellular lipid accumulation, which was used as the marker of preadipocyte-to-adipocyte differentiation, was determined by Oil red O staining. (A) 3T3-L1 preadipocytes (3T3-L1 cells cultured with normal medium); (B) 3T3-L1 adipocytes (3T3-L1 cells cultured with differentiation medium without Ad treatment); (C) 3T3-L1 cells cultured with differentiation medium with AdK7-H1 (10,000 VP/cell) treatment; (D) 3T3-L1 cells cultured with differentiation medium with AdK7-H1-PPARγ (3000 VP/cell) treatment; (E) 3T3-L1 cells cultured with differentiation medium with AdK7-H1-PPARγ (10,000 VP/cell) treatment; (F) 3T3-L1 cells cultured with differentiation medium with AdK7-H1-Scramble (10,000 VP/cell) treatment; (G) 3T3-L1 cells cultured with differentiation medium with AdK7-Null (10,000 VP/cell) treatment.

sequence of siRNA for PPARγ was selected to knockdown both PPARγ1 and PPARγ2 (Katayama et al., 2004). We confirmed by Western blotting that AdK7-H1-PPARγ suppresses the expression levels of PPARγ in 3T3-L1 adipocytes (Fig. 3). The levels of PPARγ in the cells treated with 3000 or 10,000 VP/cell of AdK7-H1-PPARγ were decreased to 51% or 16% of the levels in cells treated with AdK7-Null (10,000 VP/cells), respectively. AdK7-H1, AdK7-H1-Scramble and AdK7-Null did not show any effect on the PPARγ expression, compared with non-infected cells. These results indicated that AdK7-H1-PPARγ effectively suppressed the expression of PPARγ in 3T3-L1 cells.

3.3. Suppression of the preadipocyte-to-adipocyte differentiation in 3T3-L1 cells

During the process of preadipocyte-to-adipocyte differentiation, 3T3-L1 preadipocytes initiate the storage of energy in the form of triacylglycerol-rich lipid droplets. The degree of differentiation of 3T3-L1 cells can be evaluated by measuring the accumulation of intracellular lipids, which are stained by Oil red O, and GPDH activity. We next examined whether AdK7-H1-PPARγ suppresses the preadipocyte-to-adipocyte differentiation in 3T3-L1 cells. The 3T3-L1 cells were transduced with Ad vectors and reached confluence on the following day. Two days after reaching confluence, the cells were cultured with differentiation medium for 9 days and stained with Oil red O. Intracellular lipid accumulation was reduced in 3T3-L1 cells transduced with AdK7-H1-PPARγ (Fig. 4). The levels
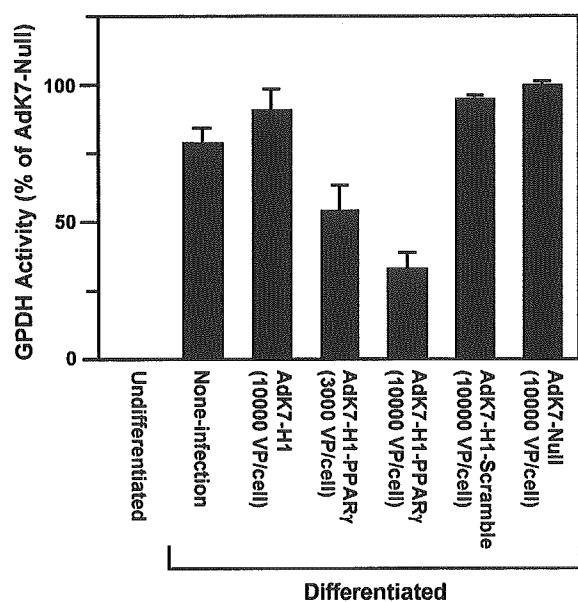

Fig. 5. Suppression of the fatty synthesis on 3T3-L1 cells transduced with AdK7-H1-PPARγ. The cells and virus were treated as described in the legends of Fig. 4. The fatty synthesis was determined by the measurement of GPDH activity in 3T3-L1 cells. Data were expressed as percentage of the GPDH activity of 3T3-L1 cells cultured with differentiation medium with AdK7-Null (10,000 VP/cell) treatment.

of GPDH activity in the cells treated with 3000 or 10,000 VP/cell of AdK7-H1-PPARγ were decreased to 55% or 33% of the levels in cells treated with AdK7-Null (10,000 VP/cell), respectively (Fig. 5). AdK7-H1, AdK7-H1-Scramble and AdK7-Null did not show any suppressive effect on the accumulation of intracellular lipid and GPDH activity (Fig. 5). These results suggested that AdK7-H1-PPARγ efficiently suppressed the preadipocyte-to-adipocyte differentiation of 3T3-L1 cells.

4. Discussion

3T3-L1 cell line is widely used for studying adipocyte differentiation and adipose biology. However, this cell line is poorly transduced by the conventional Ad vectors or DNA transfection reagents. In the present study, we successfully transduced nearly 100% of 3T3-L1 preadipocytes by using fiber-modified Ad vectors containing polylysine peptides and showed that Ad vector-mediated RNAi for PPARγ efficiently suppressed the preadipocyte-to-adipocyte differentiation. We also showed that 3T3-L1 adipocytes were efficiently transduced by the fiber-modified Ad vectors containing polylysine peptides. Carlotti et al. reported that Ad vector-mediated gene transfer into 3T3-L1 adipocytes was associated with marked cytopathogenicity (Carlotti et al., 2004). In our results, no cytotoxicity, adipogenicity, or other negative effects on cell function were observed by the Ad vector-mediated gene transfer.

Several strategies have been employed to overcome the poor transduction efficiency of 3T3-L1 cells. Because the low expression of CAR, the primary Ad receptor, in 3T3-L1 cells would the cause of the poor transduction of the conventional Ad vectors (Fig. 2), 3T3-L1 cells stably expressing CAR by the transfection have been developed (Orlicky et al., 2001; Ross et al., 2003). However, CAR is an adhesion molecule which mediates tight junctions and homotypic interactions (Honda et al., 2000; Cohen et al., 2001). Therefore, there might be negative effects of ectopic CAR expression in the process of adipogenesis of 3T3-L1 cells. Another strategy is to use transduction-enhancing agents such as polylysine, lipofectAMINE (Invitrogen Life Technologies), or SuperFect (Qiagen Inc.), which mediate CAR-independent transduction of Ad vectors (Orlicky and Schaack, 2001). These reagents sometimes negatively affect cellular function, e.g., via their cytotoxicity or their inhibition of cell growth and differentiation. Complexes of Ad vectors and transduction-enhancing agents are also non-uniform and are not likely to show reproducible results. Fiber-modified Ad vectors overcome all these problems. Among the vectors tested in the present study, polylysine-modification of the Ad fiber, which is negatively charged, exhibited the most efficient gene transfer to 3T3-L1 preadipocytes and adipocytes. This result correlates well with the report of Orlicky and Schaack that complexes of Ad vectors and polylysine enhanced transduction in 3T3-L1